San Jose State University
SJSU ScholarWorks

Master's Theses | Master's Theses and Graduate Research

2005

Reset noise in CMOS image sensors

Irene Gonzales Calizo
San Jose State University

Follow this and additional works at: https://scholarworks.sjsu.edu/etd_theses

Recommended Citation
Calizo, Irene Gonzales, "Reset noise in CMOS image sensors" (2005). *Master's Theses*. 2746.
DOI: https://doi.org/10.31979/etd.tmv5-rjer
https://scholarworks.sjsu.edu/etd_theses/2746

This Thesis is brought to you for free and open access by the Master's Theses and Graduate Research at SJSU ScholarWorks. It has been accepted for inclusion in Master's Theses by an authorized administrator of SJSU ScholarWorks. For more information, please contact scholarworks@sjsu.edu.

RESET NOISE IN CMOS IMAGE SENSORS

A Thesis

Presented to

The Faculty of the Department of Electrical Engineering

San Jose State University

In Partial Fulfillment

of the Requirements for the Degree

Master of Science

by

Irene Gonzales Calizo

August 2005

UMI Number: 1429409

Copyright 2005 by
Calizo, Irene Gonzales

All rights reserved.

INFORMATION TO USERS

The quality of this reproduction is dependent upon the quality of the copy submitted. Broken or indistinct print, colored or poor quality illustrations and photographs, print bleed-through, substandard margins, and improper alignment can adversely affect reproduction.

In the unlikely event that the author did not send a complete manuscript and there are missing pages, these will be noted. Also, if unauthorized copyright material had to be removed, a note will indicate the deletion.

UMI®

UMI Microform 1429409
Copyright 2006 by ProQuest Information and Learning Company.
All rights reserved. This microform edition is protected against unauthorized copying under Title 17, United States Code.

ProQuest Information and Learning Company
300 North Zeeb Road
P.O. Box 1346
Ann Arbor, MI 48106-1346

© 2005

Irene Gonzales Calizo

ALL RIGHTS RESERVED

APPROVED FOR THE DEPARTMENT OF ELECTRICAL ENGINEERING

7/7/2005

Dr. Lili He

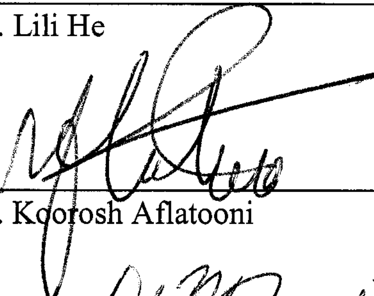

7/8/2005

Dr. Koorosh Aflatooni

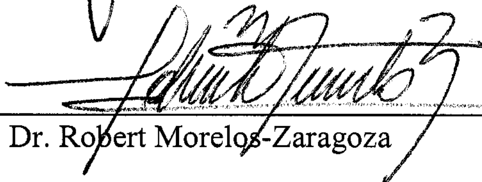

7/7/2005

Dr. Robert Morelos-Zaragoza

APPROVED FOR THE UNIVERSITY

7/29/05

ABSTRACT

RESET NOISE
CMOS IMAGE SENSORS

by Irene G. Calizo

There is a large market for imaging systems for mobile devices such as cell phones, personal digital assistants, and toys. These applications require low-power, low cost, and small size. These needs can be satisfied with a CMOS image sensor. Unfortunately, the CMOS image sensor has historically suffered from lower noise performance than the charge-coupled device (CCD).

Reset noise is a dominant source of noise for the imager, particularly in low-light level conditions. It arises from a time dependent uncertainty of charges when the pixel is reset. This affects the pixel's ability to sense low signal levels. This thesis investigates reset noise in a CMOS image sensor pixel from a mesoscopic perspective and ways to reduce reset noise including soft reset. The reset noise and soft reset of the pixel in the CMOS image sensor was simulated. Through this simulation, soft reset was found to reduce the reset noise by 40%.

ACKNOWLEDGEMENTS

First I would like to thank Professor Lili He her advice and serving on my thesis committee. I am thankful for your assistance whenever I had a problem or question, even at the last minute. You were very helpful and positive each time we talked even if you were very busy. Your comments were invaluable to me.

I am truly grateful to have the opportunity to learn from and work under Professor Koorosh Aflatooni during my graduate studies at San Jose State University. I cannot overstate my deepest gratitude for your sound advice, guidance, encouragement, and support. Thanks for taking the time and energy to explain difficult concepts to me clearly and simply. I would have been absolutely lost with you.

I would also like to thank Professor Robert Morelos-Zaragoza for providing wise advice and writing letters on my behalf.

I wish to thank everyone at Foveon Inc., for introducing me to the amazing world of CMOS image sensors. I have never been around a smarter group of people.

I want to thank my father and sister for their patience and support during my time at San Jose State University. Finally, I would like to dedicate this thesis to my late mother who always encouraged me in my studies.

Table of Contents

1 Introduction ... 1
1.1 CCD vs. CMOS Image Sensors ... 1
1.2 Reset Noise ... 2
1.3 Thesis Organization ... 3
2 Probability and Random Processes ... 4
2.1 Statistics ... 4
2.2 Bernoulli Distribution ... 5
2.3 Binomial Distribution ... 5
2.4 Poisson Distribution ... 6
2.5 Gaussian Distribution ... 6
2.6 Burgess Variance Theorem ... 7
3 CMOS Image Sensors ... 8
3.1 Sensor Types ... 8
3.2 Sensor Architecture ... 10
3.3 Pixel Structure ... 11
3.4 Pixel Operation ... 12
4 Noise in CMOS Image Sensors ... 16
4.1 Reset (kTC) Noise ... 17
4.2 1/f (Flicker) Noise ... 20
4.3 Shot Noise ... 21
4.4 Thermal Noise ... 23
4.5 Sensor Performance Parameters ... 24
4.6 CMOS Image Sensor Reset Noise Reduction ... 25
4.6.1 Correlated Double Sampling (CDS) ... 25
4.6.2 Active Reset ... 26
4.6.3 Depleted Photodiode ... 28
4.6.4 Pinned Photodiode ... 29
4.6.5 Soft Reset ... 30
5 Reset Noise from a Mesoscopic Perspective ... 32
5.1 Thermionic Emission (TE) in a p-n diode ... 33
5.2 Coulomb blockade effect ... 33
5.3 Operational Regimes ... 34
5.3.1 Mesoscopic (Coulomb Blockade) Regime ... 35
5.3.2 Sub-Poisson Regime ... 36
5.3.3 Poisson Regime ... 36
5.3.4 Macroscopic Regime ... 36
5.4 Probability of Thermionic Emission ... 37
5.5 Collective vs. single electron coulomb blockade regime ... 38
6 Monte Carlo Simulation of Reset Noise ... 40
6.1 Monte Carlo simulation of p-n diode thermionic emission ... 41
6.2 Monte Carlo simulation of reset noise in CMOS image sensor pixel ... 47

6.3 Results and Discussion 52
7 Conclusion 55
7.1 Future Work 55
Appendix A: MATLAB® Code 56
References 76

List of Figures

Fig. 3.1 Standard 3 transistor pixel structure for a CMOS image sensor. 9
Fig. 3.2 Standard 4 transistor pixel structure in a CMOS image sensor. 10
Fig. 3.3 CMOS Image Sensor Architecture 11
Fig. 3.4 Color filter pattern used in a typical pixel array. 12
Fig. 3.5 Pixel operation timing diagram showing the relation between the photodiode voltage and the reset and row select transistors. 13
Fig. 3.6 Timing diagram showing read and reset for rolling shutter in CMOS image sensor. 15
Fig. 4.1 Typical voltage response versus optical power of a color channel. Imager performance at low light levels is limited by noise floor. 17
Fig. 4.2. Photodiode connected to reset transistor showing equivalent capacitance, C, and resistance, R. 18
Fig. 4.3 Timing diagram showing photodiode voltage fluctuations due to pixel reset noise. 19
Fig. 4.4 1/f noise and determination of corner frequency. 21
Fig. 4.5 Shot noise which can be found in the CMOS image sensor. 22
Fig. 4.6 Thermal noise found in a resistor. 24
Fig. 4.7 CMOS image sensor pixel for Active Reset [8] 27
Fig. 4.8 Active reset timing diagram [8]. 28
Fig. 4.9 Schematic of pinned photodiode [15]. 29
Fig. 5.1 Junction voltage vs. time for mesoscopic p-n junction with constant current source[17]. 35
Fig. 6.1 Algorithm used in simulation thermionic emission in pn diode. 42
Fig. 6.2 Simulated junction voltage vs. time for thermionic emission in a p-n diode with constant current. 46
Fig. 6.3 Simulated junction voltage vs. time for thermionic emission in p-n diode with voltage dependent current. 46
Fig. 6.4 Algorithm used to simulate reset noise in CMOS image sensor pixel. 48
Fig. 6.5 Histogram of conventional reset noise in CMOS image sensor pixel. 49
Fig. 6.6 Simulation of conventional reset noise in CMOS image sensor pixel. 50
Fig. 6.7 Histogram of highest sense node voltages for soft reset. 51
Fig. 6.8 Simulated highest sense node voltage vs. time in CMOS image sensor pixel for soft reset. 52

List of Tables

Table 1 CCD versus CMOS image sensor technology. 2
Table 2 Simulation parameters for pn diode. 41
Table 3 Simulation parameters used for voltage controlled current. 44

1 Introduction

1.1 CCD vs. CMOS Image Sensors

Two technologies are in use today to produce image sensors, charge-coupled device (CCD) and the CMOS image sensor. CCDs were first developed in the 1970's and represent a mature technology with excellent performance and the ability to produce high quality images. Although the CMOS image sensor was already in existence during that time, low performance prohibited its use in imaging systems. Not until the 1990's had their quality improved enough that they could be used in low-end applications. Noting the advantages of using a CMOS process over CCD, much work was put into improving their performance. Today CMOS image sensors are on their way to overtake the CCD as the technology of choice in imaging systems. A number of companies are already making high quality image sensors for professional level digital cameras.

CMOS image sensors owe their growth in popularity to several factors. These include low power consumption, low voltage operation, system electronics integration, and low cost due to worldwide fab availability [1]. CCDs, which have high capacitances, require a lot of power because they need multiple clocks with large voltages. While the CMOS image sensor uses much fewer power supplies at lower voltages. A CCD needs a separate chip for image processing and other electronics since the CCD process is highly specialized and not fabricated along with CMOS chips. On the other hand, the CMOS image sensor can include all electronics on a single chip making possible a complete camera-on-chip system. The drawback of this is that the overall chip becomes more complex and it may make more sense to use two chips to improve imager performance.

These advantages make CMOS image sensors ideal for such applications as digital cameras, cell phones, PDA's, and toys.

Table 1 CCD versus CMOS image sensor technology.

	CCD	*CMOS*
Power consumption	hi	low
Cost	high	low
Size	large	small
Noise	low	high
Integration with CMOS	No	yes
Scalability	yes	better than CCD
Fabrication	Specialized process	Common process
Voltage levels needed	many	few

1.2 Reset Noise

As CMOS technology has moved to smaller design rules, reset noise has become a limiting factor in pixel performance [2-3]. The purpose of a reset operation is to provide a reference level for comparison with the number of electrons generated from photons incident to the photodiode. Reset noise originates from thermal noise causing voltage fluctuations in the reset level for a pixel. A noisy reset operation can affect the pixel performance especially in low light level conditions because of an increased noise floor. As the dimension of pixels shrinks, reset noise becomes dominant where misplacements of a single electron can generate 50 μV of noise across a capacitance of 3 fF, typically

found in modern CMOS pixel architectures. This is a significant change in voltage compared to the generated signal, which in turn will negatively impact the imaging performance.

Traditionally, a hard reset is used to reset the pixel. During a hard reset, the gate voltage is made greater than the drain voltage plus the threshold voltage of the reset transistor. The role of the reset transistor is like a switch that charges up the sense node to VDD. On the other hand, for a soft reset, the gate and drain are placed at VDD. Therefore the reset transistor will be weakly inverted. The resulting sub-threshold current in the reset transistor is used to reset the sense node logarithmically beyond VDD – $V_{T,rst}$. Some recent publications claim a soft reset of a photodiode CMOS image sensor pixel will lead to lower reset noise.

1.3 Thesis Organization

Chapter 2 of this thesis provides some mathematical background in probability theory used in studying noise. Chapter 3 provides a brief overview of CMOS image sensors. Noise in semiconductor devices and CMOS image sensors is discussed in Chapter 4. Chapter 5 presents reset noise from a mesoscopic perspective. Monte Carlo Simulation of reset noise along with the results of the simulation is discussed in Chapter 6. Chapter 7 is the conclusion of the thesis.

2 Probability and Random Processes

Since electron energies in a p-n junction are randomly distributed, the electrical characteristics, like current and voltage, produced with these devices will do so as well. Reset noise appears as an unpredictable function of time which can be characterized in terms of its statistical properties. This chapter will provide an overview of the probability theory used to model and simulate reset noise

2.1 Statistics

Familiar statistics such as mean, standard deviation, and variance can be used to describe noise. The standard deviation is representative of the value of the noise. The mean, or expected value, $E[X]$, is given by [4]

$$E[X] = \int_{-\infty}^{\infty} t f_X(t) dt \tag{1}$$

Where X is a continuous random variable and t is time. The mean is usually zero so the standard deviation and variance provide better descriptions of noise. The standard deviation relates how tightly the distribution is about the mean. If the standard deviation is high, then the data is differing more from the average as compared to a low standard deviation. The standard deviation, $\sigma[X]$, is given by [4]

$$\sigma[X] = \sqrt{E\left[(X - E[X])^2\right]} \tag{2}$$

The variance illustrates the spread of the distribution and is just the square of the standard deviation, $\sigma^2[X]$.

2.2 Bernoulli Distribution

The Bernoulli distribution is used to describe a success in a series of independent events. Each time the experiment is completed, it is referred to as a Bernoulli trial. Since the same experiment is repeated, then each trial has the same probability of a successful outcome. A random number variable, $I_A(\xi)$, indicates whether an event, A, did or did not occur. If A occurred, we call it a success and the random variable $I_A(\xi)=1$. If A did not occur, it was a failure and the random variable $I_A(\xi)=0$. After tossing a coin repeatedly, the distribution will be a Bernoulli. If k is the number of success in n trials, the probability mass function (pmf) is [4]

$$p(0) = 1 - p \quad \text{and} \quad p(1) = p \quad \text{for } 0 \le p \le 1 \tag{3}$$

where $P[A] = p$ and 1 indicates the event occurred and 0 indicates the event did not occur. A Bernoulli random process is an independent, identically distributed sequence of Bernoulli random variables. Its mean and variance are [4]

$$E[X] = p \tag{4}$$

$$\sigma^2[X] = p(1-p) \tag{5}$$

2.3 Binomial Distribution

The binomial distribution consists of an experiment with n independent identical trials. For an event, A, the outcome is either a success or a failure. Binomial distributions are useful in describing events where there are two possible outcomes and you would like to find how many times one of those outcomes occurred out of n times. Let X be the number of successful outcomes of event A. Then the pmf is given by [4]

$$p_k \quad = \quad \binom{n}{k} p^k (1-p)^{n-k} \; k = 0,\ 1,\ 2, \ldots, n \tag{6}$$

2.4 Poisson Distribution

The Poisson distribution can be used to describe arrivals as a function of time. An example of this is the arrival of electrons on the sense node of the pixel. It represents how many times a random event, A, occurs out of a certain number of times (trials). The probability of exactly n successes in N trials of an event with probability p is given by [5]

$$W(n) = \frac{N!}{n!(N-n)!} p^n (1-p)^{N-n} \tag{7}$$

For the case of the binomial distribution in which p is much less than one and the number of successes is much less than the number of trials, the binomial distribution can be approximated by Poisson distribution. This probability that an event occurs n times for a large number of trials is known as the Poisson distribution and is given by [5]

$$W(n) = \frac{\lambda^n}{n!} e^{-\lambda} \tag{8}$$

where $\lambda \equiv N p$ and is the mean number of times the event occurs.

2.5 Gaussian Distribution

In many instances, when dealing with a large number of events, the distribution is Gaussian. This is especially true for other types of noise like 1/f noise and shot noise that have a Gaussian distribution. The Gaussian pdf is given by [5]

$$f(x) = \frac{1}{\sqrt{2\pi\sigma^2}} e^{\frac{-(x-a)^2}{2\sigma^2}} \tag{9}$$

where a is the mean and σ is the standard deviation.

2.6 Burgess Variance Theorem

The Burgess variance theorem is used to describe the variance of a Bernoulli process when both the number of trials and outcome varies. The Bernoulli process, $P_k(k_o)$, described as the probability of k_o successes in n trials is given by [6]

$$P(k_o) = \sum_{n=k}^{\infty} W(n) P_k(k_o) \tag{10}$$

where $W(n)$ describes the distribution of the total number of trials and $P_k(k_o)$ is the probability of k_o successes in n total trials. The variance in the number of successes is given by the Burgess variance theorem [6]

$$\sigma_{k_o}^2 = \sigma_n^2 P^2 + \bar{n} P(1-P) \tag{11}$$

where $\sigma_n^2 = \overline{n^2} - \bar{n}^2$.

3 CMOS Image Sensors

Before CMOS image sensors, charge-coupled device (CCD) image sensors were the dominant sensor used in digital imaging systems. But CCDs require a specialized fabrication process which makes them expensive to manufacture. These wafer fabs can then only be used to produce CCDs. On the other hand, the CMOS process is the most popular, being used today to produce a great percentage of all the semiconductor chips worldwide. As a result, the CMOS image sensor can be made in the same foundry as most other semiconductor chips.

With the emergence and the recent growth of the CMOS image sensor market, a number of companies have leveraged their RAM process technology expertise to enter the CMOS image sensor market, producing high quality CMOS image sensors. A CMOS process allows the image sensor to be integrated with other imaging electronics to produce a complete camera-on-chip. This not only reduces size but also cost. CCDs require much more power than CMOS image sensors. This combined with its ability to scale with VLSI technology, make it a natural choice for mobile applications such as camera phones.

3.1 Sensor Types

The two most common sensor types are the three transistor active pixel sensor (3T APS) and the four transistor active pixel sensor (4T APS) with schematic shown in Fig. 3.1 and Fig. 3.2. Active pixel sensors include a source follower transistor in every pixel whose amplification improves noise. The extra transistor in the 4T pixel acts like a

shutter. When the Reset and the Tr transistor are turned on, the photodiode is reset. The reset operation ends when the reset transistor is turned off.

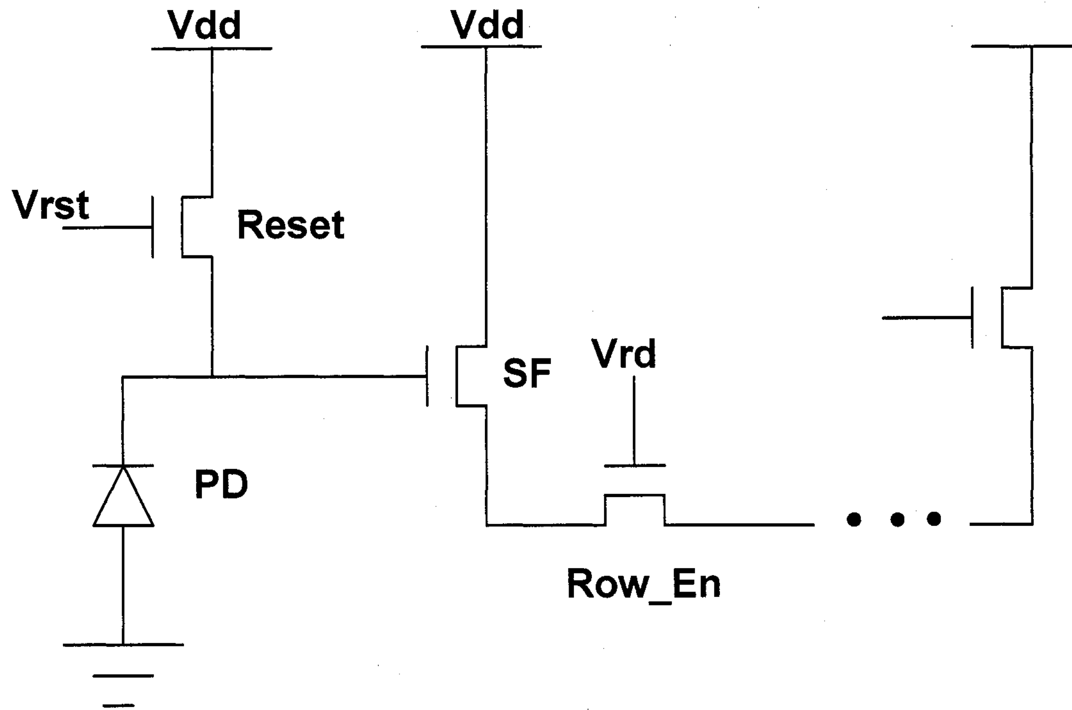

Fig. 3.1 Standard 3 transistor pixel structure for a CMOS image sensor.

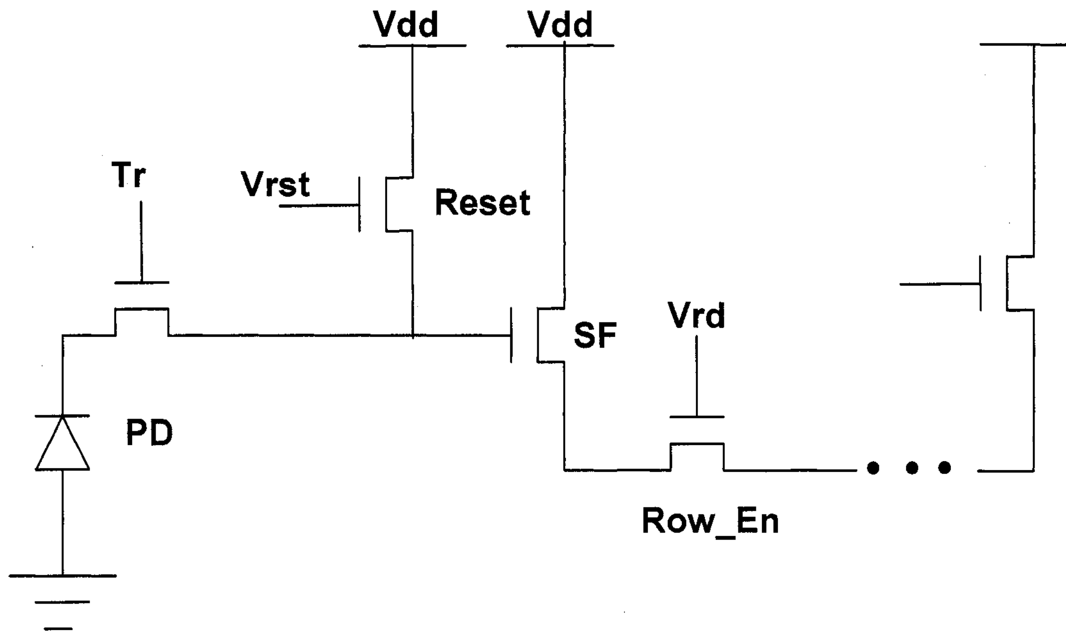

Fig. 3.2 Standard 4 transistor pixel structure in a CMOS image sensor.

3.2 Sensor Architecture

The basic CMOS image sensor architecture is shown in Fig. 3.3. The pixel array converts incoming photons into electron charge. The row decoding lines select a row of pixels. The column lines read a particular pixel in the row for output. Signal processors can provide gain and other improvement functions. On-chip analog to digital converters in addition to digital control and interface circuitry are included.

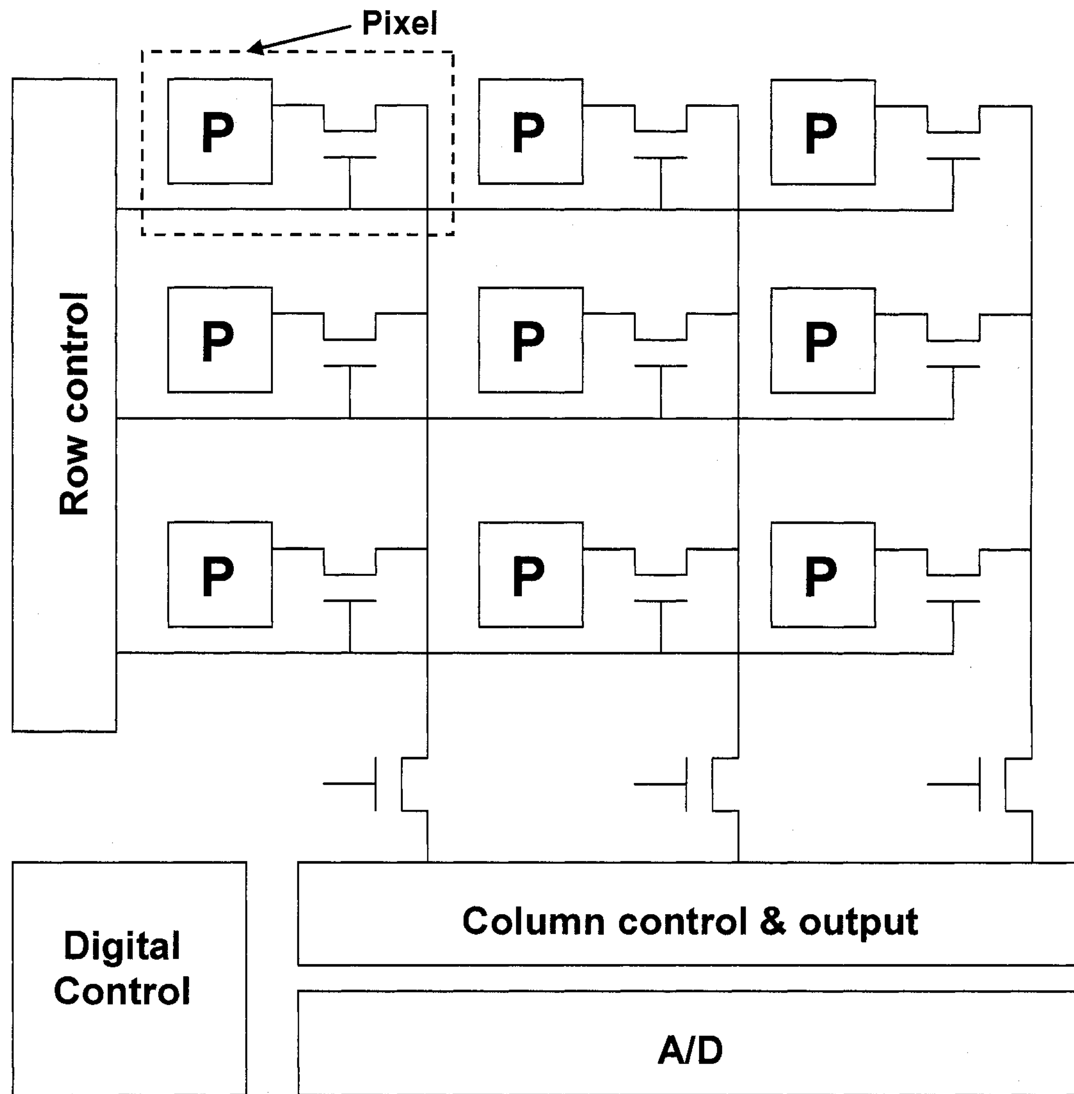

Fig. 3.3 CMOS Image Sensor Architecture

3.3 Pixel Structure

The standard 3T pixel in Fig. 3.1 consists of a photodiode connected to a reset transistor, a source follower, and a row enable transistor. A typical pixel will have either a red, green, or blue color filter over it in order to sense one of the three colors. The

filters are arranged over the pixel array in a three color checkerboard fashion such as the popular Bayer mosaic pattern depicted in Fig. 3.4. The detector records the intensity of the light and uses the color filter to extract one color component. One drawback of this method is that it reduces optical resolution by one third since each photodiode is sensing one color.

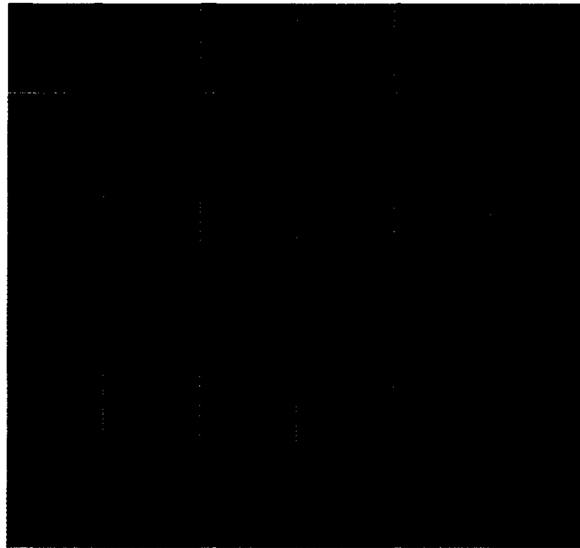

Fig. 3.4 Color filter pattern used in a typical pixel array.

3.4 Pixel Operation

The pixel timing diagram is shown in Fig. 3.5. The photodiode is first reset by turning on the reset transistor. The previous charge from the photodiode is removed and then the photodiode capacitance is charged to a predetermined value which reverse biases the photodiode. In a hard reset, the gate voltage of the reset transistor is greater than the drain voltage by more than its threshold voltage. The transistor acts like a switch and the photodiode will be charged up to the drain voltage.

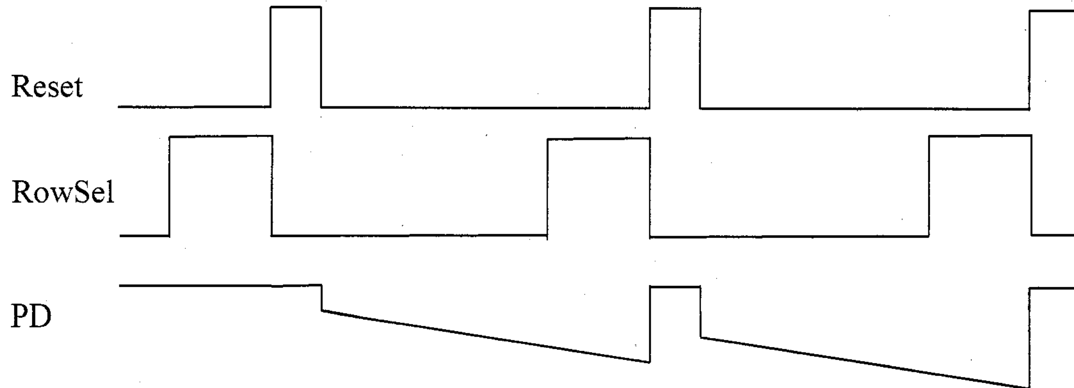

Fig. 3.5 Pixel operation timing diagram showing the relation between the photodiode voltage and the reset and row select transistors.

Integration time is controlled by the reset transistor. It begins when the reset transistor is turned off and ends when it is turned back on. During the integration time, photons incident on the active region of the pixel will be absorbed by electrons in the valence band. These valence band electrons will be excited to the conduction band if the incident photon's energy is at minimum equal to the semiconductor's band gap energy. This creates electron-hole pairs producing a current. By reverse biasing the diode, the diode's depletion region as well as its electric field will increase which prevents the conduction band electrons from recombining with holes by sweeping them away across the depletion region and onto external circuitry.

Integration time is analogous to exposure time in a conventional film camera. The time of integration should be long enough to collect enough photons to convert to electrons therefore detecting the incoming light Too long an integration time will result in saturated data. During integration the photodiode, essentially a capacitor, is discharged. Therefore a low light level pixel results in a high voltage signal.

After reset and integration, the pixel data can be read out. This occurs row by row in a rolling as shown in Fig. 3.6. A high signal is given to the first row enable line in the array of pixels, this is when the row is read out. After time t_{roll} , the second row will given a high row enable signal. Similarly after some time t_{int} , after the first row's row enable line went high, the first row's pixel reset line will be made high to reset the pixel and the row enable line is made low. Time t_{roll} after that point, the second row will be given a high reset signal. This will select a particular pixel from the pixel array to output the data to the signal processing circuitry. A CMOS image sensor can also employ a global shutter operation which allows the whole pixel array to integrate and then read out at the same time. This allows images to be taken faster than with a rolling shutter. This technique requires an additional transistor which acts as a shutter between the source of the reset transistor and the gate of the source follower.

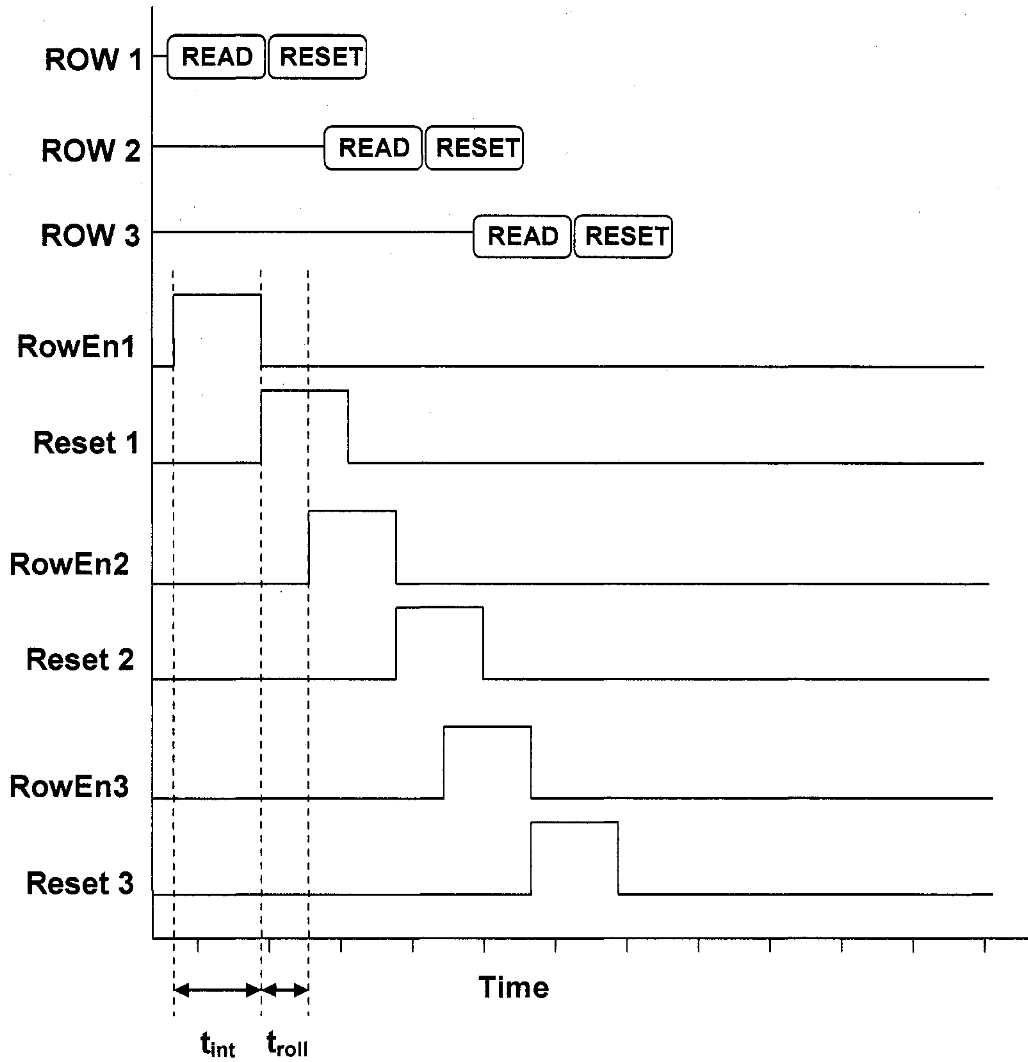

Fig. 3.6 Timing diagram showing read and reset for rolling shutter in CMOS image sensor.

4 Noise in CMOS Image Sensors

Noise is present in any semiconductor device. Its cause can range from fabrication process imperfections to the random nature of charge carriers in the device. Because noise in solid state devices is a random process, it is best described by its statistics. For CMOS image sensors in particular, noise can have an adverse effect on its ability to sense low voltages and result in poor image quality. In order to improve an imaging system's image quality, CMOS image sensor companies have faced increasing pressure to limit noise in CMOS image sensors.

Noise in a CMOS image sensor can be categorized as temporal or fixed pattern noise (FPN). Fixed pattern noise can occur from not matching perfectly the threshold voltages of the transistors in the pixel array, interconnect mismatching, and differences in the column transistor's capacitors among other effects. These transistors include the reset, source follower, row enable, and column connection to pre-charge as shown in Fig. 3.1. This threshold voltage mismatch results in different gain values for these transistors which produces differences in the output from pixel to pixel when equally illuminated. FPN noise can be further classified as offset FPN and photo response non-uniformity (PRNU). Offset FPN changes between sensor arrays but not between frames. PRNU is seen as a non-uniform slope in a pixel's photo-response curve.

The fundamental limit of imager performance is set by the temporal noise [7]. Sources of temporal noise are 1/f, shot, reset noise, and thermal noise of the source follower, access, and reset transistor of the pixel [7]. Reset noise is the largest source of temporal noise [8].

The noise floor of a sensor will determine the lowest value it can read. Therefore, the lower the noise floor, the less light is needed for the image sensor to read a correct value. Fig. 4.1 shows a plot of the typical voltage response of a pixel color channel for increasing optical power. It shows that the noise will place a lower limit on the ability for the pixel to sense incoming light. Any value below the noise floor level, also called read noise, will appear as noise.

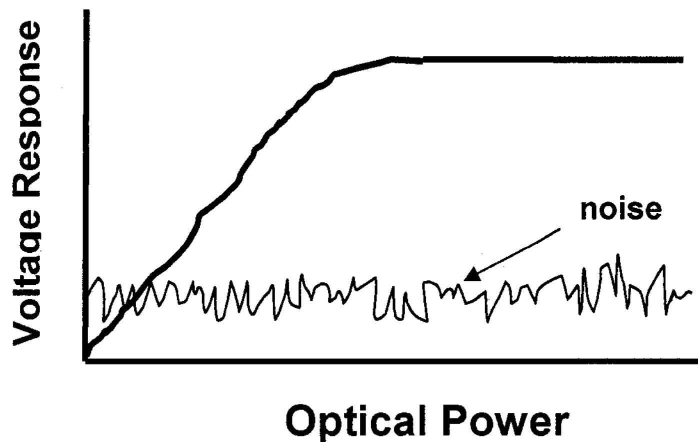

Fig. 4.1 Typical voltage response versus optical power of a color channel. Imager performance at low light levels is limited by noise floor.

4.1 Reset (kTC) Noise

In a pixel, the photodiode connected to a reset transistor is analogous to a capacitor that is charged up through a field effect transistor (FET), which is essentially a resistor controlled by its gate voltage as shown in Fig. 4.2.

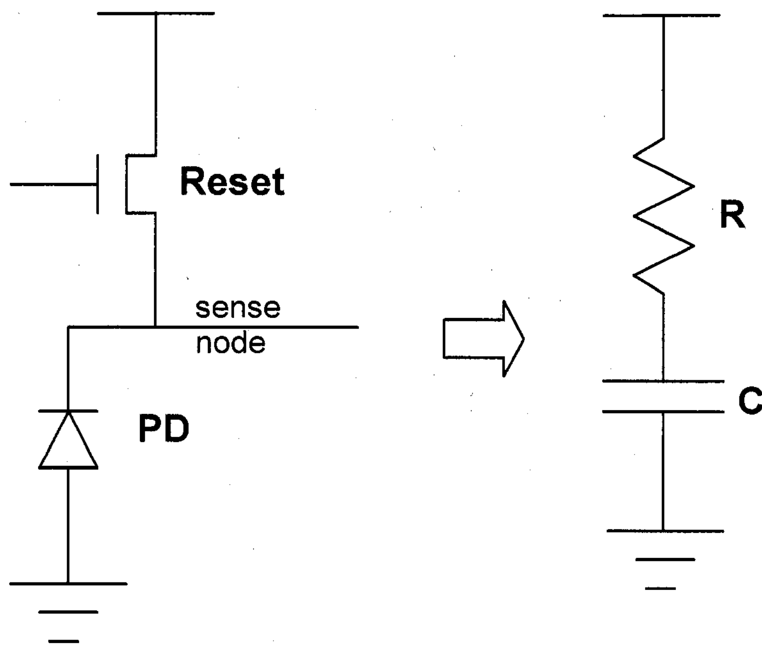

Fig. 4.2. Photodiode connected to reset transistor showing equivalent capacitance, C, and resistance, R.

For a reset operation, the Vdd is placed on the gate of the reset transistor. If the voltage on the sense node is sufficiently low, then the reset transistor will be in saturation. A high enough voltage on the sense node means that the reset transistor will be in the sub-threshold region. As the reset transistor in the pixel is turned on, it charges up the capacitor, ending up in sub-threshold. However, due to the time dependent uncertainty in the number of electrons on the sense node during reset, charges randomly arrive and leave the sense node. The random fluctuations in the amount of charge on the sense node during reset results in a corresponding photodiode reset voltage fluctuation as illustrated in Fig. 4.3. Since the photodiode's voltage is reset to a reset voltage prior to the integration time, this reset noise represents a floor in the lowest signal the photodiode can

sense. Therefore in order for the pixel to sense in low-light conditions, low reset noise levels are necessary.

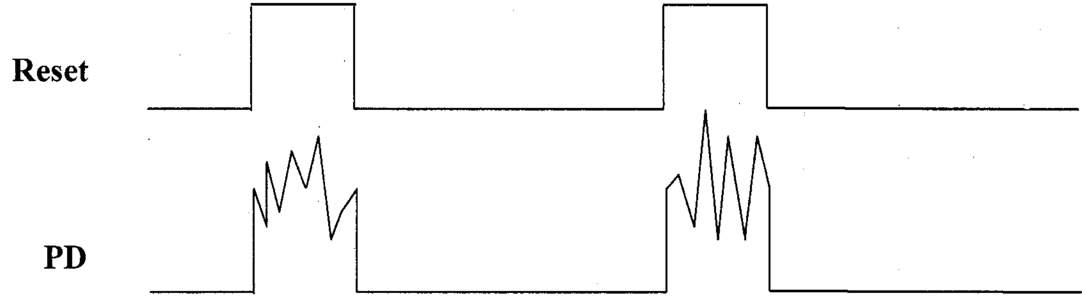

Fig. 4.3 Timing diagram showing photodiode voltage fluctuations due to pixel reset noise.

The equipartition theorem predicts that the average noise, called reset noise, depends on the temperature and capacitance and is given by [9]

$$V_{rms} = \sqrt{\frac{kT}{C}} \tag{12}$$

A capacitor's charge is related to its voltage by

$$Q = CV_{rms} \tag{13}$$

where Q is the amount of charge on the capacitor. If q is the charge of one electron, the noise can be expressed in terms of the number of electrons of capacitor noise as

$$n_{rms} = \frac{\sqrt{kTC}}{q}. \tag{14}$$

where k is Boltzmann's constant, T is absolute temperature, and C is the sense node capacitance. Its capacitance includes the photodiode's capacitance as well as parasitic capacitances from the reset and source follower transistors.

4.2 1/f (Flicker) Noise

As its name implies this type of noise is frequency dependent, with its noise power spectral density inversely proportional to frequency. Therefore it is most dominant at low frequencies, usually in the range of 1Hz to 10 kHz, appearing from impurities. For semiconductor devices, this dependence is due to traps but depends on other properties like fluctuations in mobility due to lattice scattering [10]. For example, in a MOSFET a carrier found in the channel can tunnel through the oxide to a trap. Furthermore, damage to the crystal produces a significant increase in 1/f noise because the defects produce states below the conduction band [10]. The mean-square noise current per unit bandwidth is [11]

$$\overline{i^2} = K\left(\frac{I^a}{f^n}\right)df \tag{15}$$

where K is a constant which depends on the material, I is the average dc current, a is close to 2, and n is close to 1. If a straight line is made for the slope of the 1/f noise and another straight line is made for the thermal noise floor, the frequency at the intersection of the two lines is the corner frequency, f_c, as shown in Fig. 4.4. At frequencies greater than f_c, 1/f noise becomes frequency independent and displays characteristics of thermal noise.

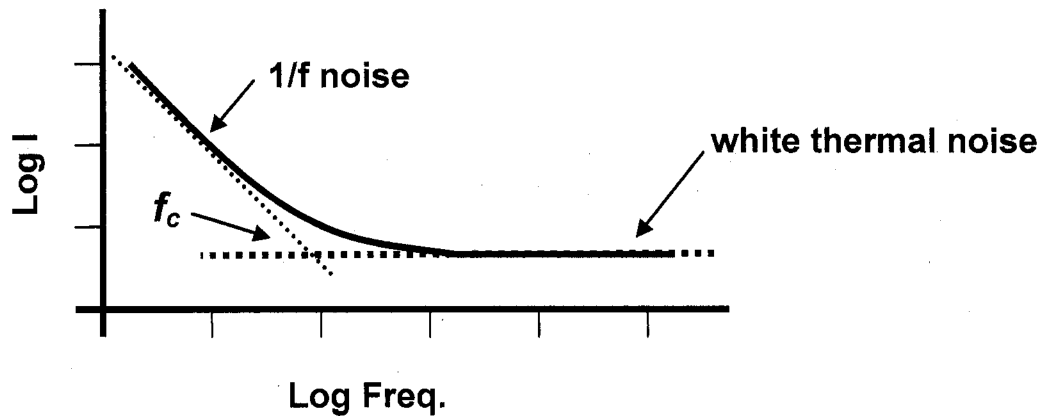

Fig. 4.4 1/f noise and determination of corner frequency.

For a CMOS image sensor, 1/f or flicker noise is associated with the sensor's readout circuit. For the pixel's NMOS, traps at the interface of the silicon and oxide produce 1/f noise. This means that this noise will be reduced if the pixel rate increases. 1/f noise contributes to the read noise of the image sensor. One method of reducing 1/f noise in CMOS imagers is to use a buried layer to increase the distance from the silicon and oxide interface.

4.3 Shot Noise

Shot noise is present in most solid state devices including p-n diodes. Observations of electronic shot noise dates back to the days of vacuum tubes. Since current is due to the movement of charged particles, the current experiences random fluctuations which is shot noise. It is consistent with carriers being emitted or crossing a potential barrier. Fig. 4.5 shows a plot of shot noise.

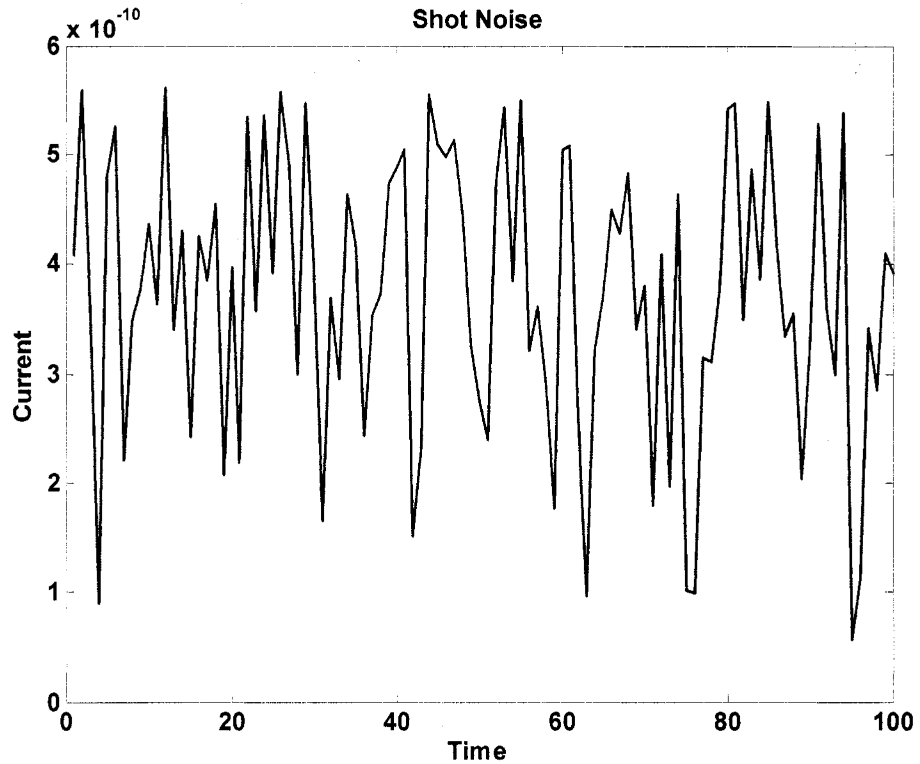

Fig. 4.5 Shot noise which can be found in the CMOS image sensor.

Since electrons are being produced randomly and independently by the photodetector, shot noise has a Poissonian distribution. The shot noise power spectral density is given by [12]

$$S_i(\omega) = 2qI \tag{16}$$

where q is the absolute value of electron charge and I is the mean current and represents the Poissonian limit. It is independent of frequency.

For an image sensor, shot noise appears because of dark current and photocurrent during the integration time. Dark current in the photodiode is the current present in the photodiode under no illumination which produces shot noise. It can result from defects or impurities in the device which gives rise to intermediate states in the bandgap,

allowing an electron into the conduction band. Photocurrent shot noise is shot noise from the photodiode due to the generated photocurrent when the photodiode is illuminated. It can occur from random arrival of photons onto the photodiode which produces a random voltage on the sense node.

4.4 Thermal Noise

Thermal noise in semiconductor devices, also known as Johnson-Nyquist noise, is dependent on temperature and type of semiconductor material. Electrons in a resistive material exhibit a Brownian motion due to collisions with the lattice as can be found in the induced channel of a MOS transistor. Therefore an electron's movements can be described by a random walk, where a step in any direction is equally likely. It may be measured as the current at the contacts of a resistor without an applied voltage and is shown in Fig. 4.6. The fact that it exists without the presence of an applied voltage is what differentiates it from shot noise and it is found in any resistor with a temperature greater than absolute zero. The open circuit noise voltage power spectral density is given by [12]

$$S_v(\omega) = 4kTR \tag{17}$$

where R is the resistance. Likewise, the short circuit noise current power spectral density is given by [12]

$$S_i(\omega) = 4kTG \tag{18}$$

where G is the conductance. In a CMOS image sensor, there is thermal noise due to the readout circuit.

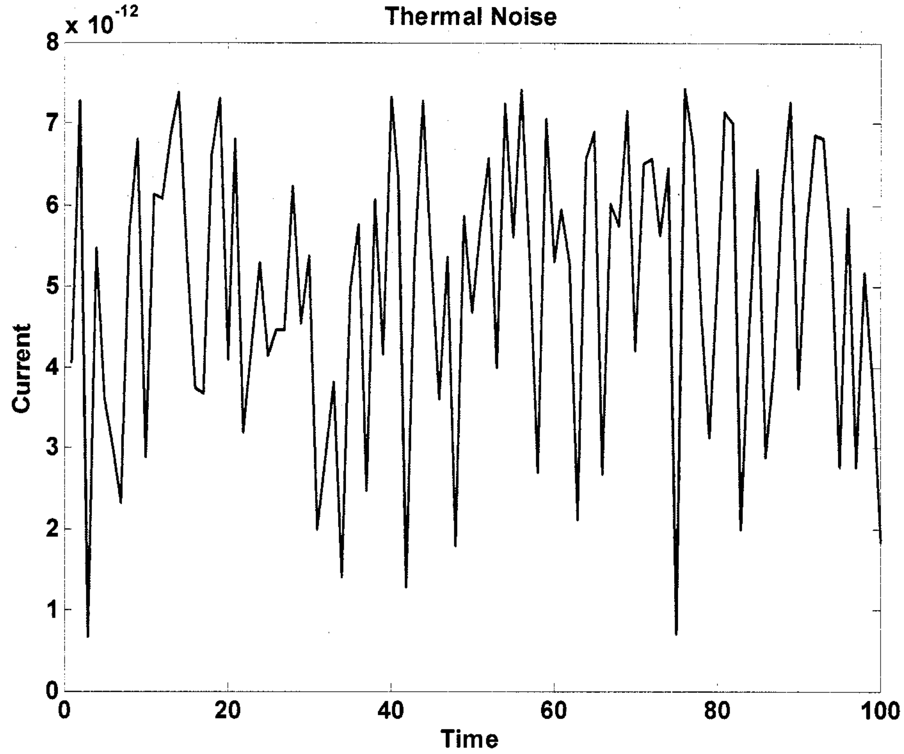

Fig. 4.6 Thermal noise found in a resistor.

4.5 Sensor Performance Parameters

Signal to noise ratio (SNR) is a figure of merit describing the imager's overall performance. For a simple camera system illuminated with a uniform light source, SNR is given by [13]

$$\left(\frac{S}{N}\right)_{FF} = \frac{4\times10^{11} QE_I P_A T_C T_L L_{UX} t_I \left(1+4f^2\right)^{-1}}{\left(N_R^2 + S_{SN}^2 + D_{SN}^2 + S_Y^2 + Q_N^2 + R^2 + N_A^2 + P_{FPN}^2 + D_{FPN}^2 + O_{FPN}^2\right)^{1/2}} \qquad (19)$$

Where Q_{EI} is the quantum efficiency of the sensor, P_A is the area of the pixel (cm^2), T_C is transmission of the pixel's color filter, T_L is transmission of the lens, LUX is light

intensity (lux), t_I is integration time (sec), f is the imaging system's lens f-number, N_R is reset noise, S_{SN} is signal shot noise, D_{SN} is dark-current shot noise, S_Y is system noise, Q_N is the analog-to-digital-converter quantization noise, R is read noise, N_A is noise from the pre-amplifier, P_{FPN} is the pixel-to-pixel FPN, D_{FPN} is dark-current FPN, and O_{FPN} is offset FPN. In reality, images are not illuminated uniformly and SNR will be less than given by (19).

4.6 CMOS Image Sensor Reset Noise Reduction

As the limiting factor in pixel performance, a number of reset noise reduction techniques have been actively pursued. Among them are correlated double sampling (CDS), active reset, depleted photodiode, pinned photodiode, and soft reset. Some methods aim to reduce the capacitance while others attack reset noise in the way the pixel is operated, each method having their own advantages and disadvantages.

4.6.1 Correlated Double Sampling (CDS)

CDS was first introduced in the 1970's to reduce the reset noise in CCDs but is now also used for CMOS image sensors. Correlated double sampling samples the photodiode's value after reset and after the integration time. The diode's value after reset represents reset noise. The second value represents reset noise plus the voltage from the image. The charges in units of electrons after reset, S_1, is given by [14]

$$S_1 = Q_{reset} + Q_{1,read} + Q_{FPN} \tag{20}$$

where Q_{reset} is the reset noise, $Q_{1,read}$ is the readout circuit noise after reset, and Q_{FPN} is offset FPN. The charges after integration in electrons, S_2, is given by [14]

$$S_2 = (i_{ph} + i_{dc})t_{\text{int}} + Q_{shot} + Q_{reset} + Q_{2,read} + Q_{FPN} + Q_{DSNU} + Q_{PRNU} \quad (21)$$

where i_{ph} is the photocurrent, i_{dc} is the dark current, t_{int} is the integration time, Q_{shot} is the integrated shot noise, $Q_{2,read}$ is the readout circuit noise at the end of integration, Q_{DSNU} is dark signal non-uniformity, and Q_{PRNU} is gain FPN. Subtracting the noise from the signal after integration gives the signal without reset noise in electrons as follows [14]

$$(S_1 - S_2) = (i_{ph} + i_{dc})t_{\text{int}} + Q_{shot} - Q_{1,read} + Q_{2,read} + Q_{DSNU} + Q_{PRNU} \quad (22)$$

Reset noise and offset FPN have been eliminated however read noise power increases. In addition, CDS cannot be used in 3 transistor pixel structures [14].

4.6.2 Active Reset

Active reset, introduced by B. Fowler et al. in [8], uses band-limiting and capacitive feedback to decrease reset noise. The authors claim a reset noise reduction to less than $kT/18C$ with this method. An active reset pixel differs from the pixel represented in Fig. 3.1 in that it includes additional circuitry to control a reset operation. The pixel structure as presented in [8] is shown in Fig. 4.7. The pixel described in [8] requires an op amp and two additional transistors. Transistors M2 and M3 are the readout transistors and M1, M4, and M5 are the reset transistors.

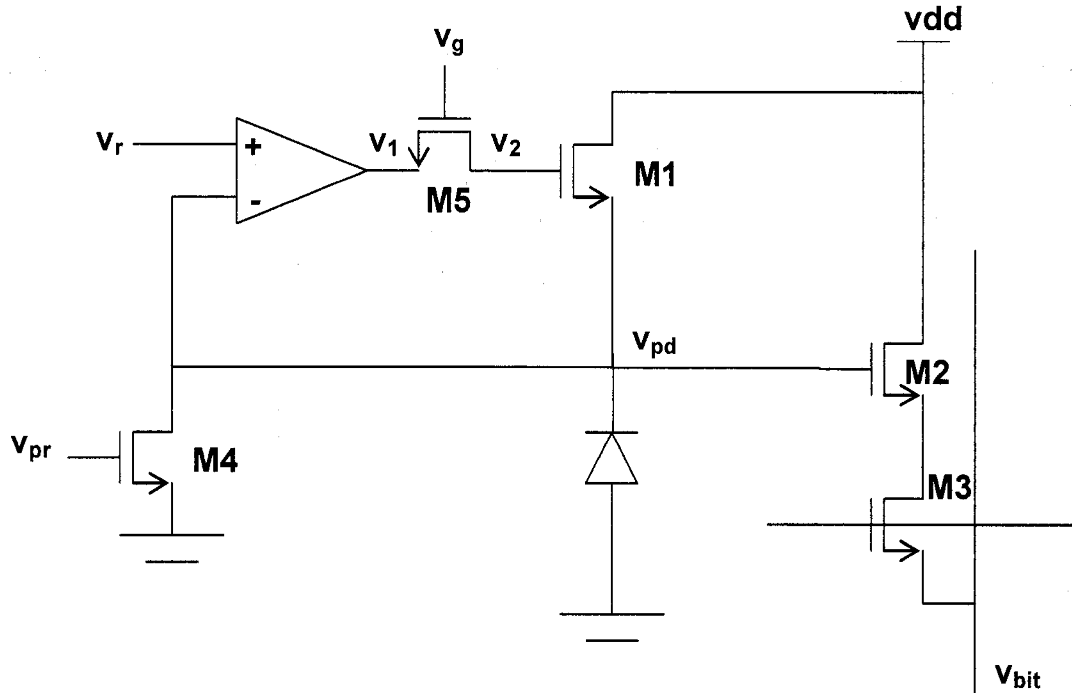

Fig. 4.7 CMOS image sensor pixel for Active Reset [8]

The timing diagram for Active reset is shown in Fig. 4.8. Reset operation begins by giving a short pulse to v_{pr} which pulls v_{pd} to ground. After this pulse v_{dd} is applied to v_g. With M5 now on, v_r slowly increases from ground to its high voltage. Not until v_r is greater than v_{pd} will the output of the amplifier be high enough to turn on M1. v_{pd} will follow v_r until it stops increasing and v_{pd} passes v_r. At this point, the op-amp output decreases and causing M1 to turn off. In the last step of this reset operation, v_g falls and M5 turns off. The tradeoffs associated with this method are a larger pixel, longer reset time, and greater power consumption.

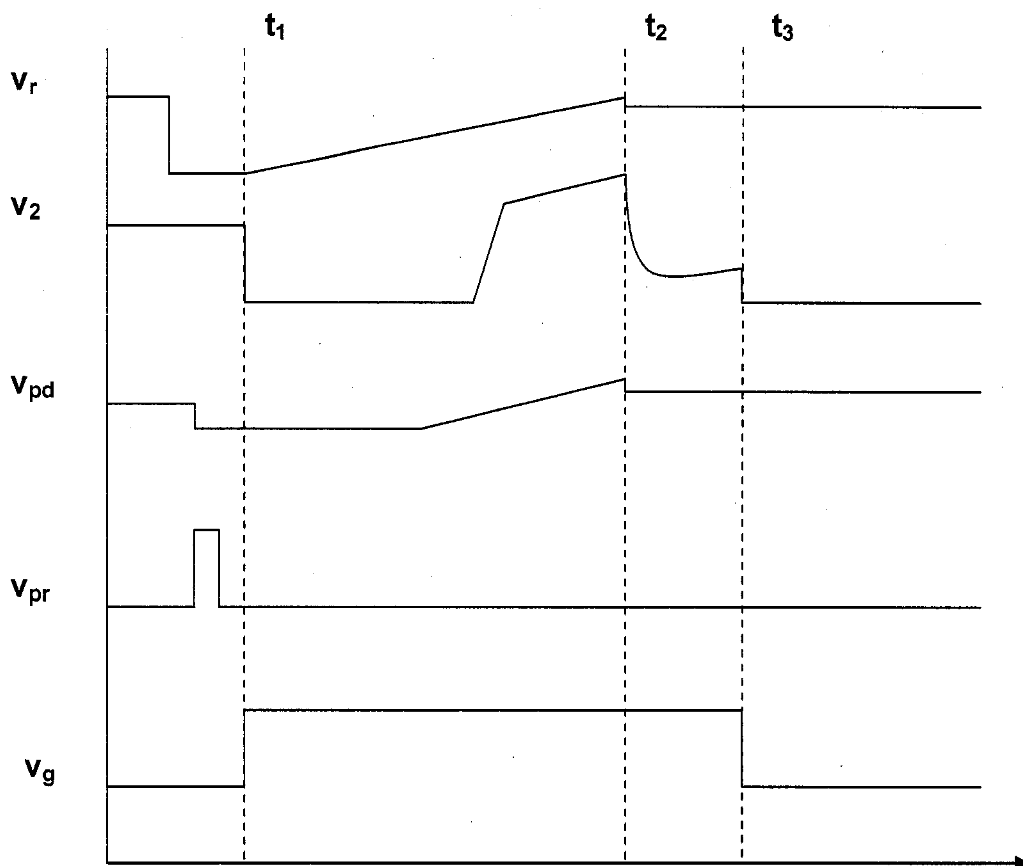

Fig. 4.8 Active reset timing diagram [8].

4.6.3 Depleted Photodiode

The goal of a fully depleted photodiode is to make the junction capacitance as low as possible. The capacitance of the junction decreases as the width of the depletion region increases. The larger the depletion region, the lower the junction capacitance will be. A fully depleted diode will have its depletion region extending all the way to the back of the diode. Since kTC noise increases with increasing capacitance, the lower junction capacitance will lower kTC noise. In order to fully deplete the diode, the photodiode

must have a large applied reverse bias. However, this also results in an increase in dark current.

4.6.4 Pinned Photodiode

Another technology taken from CCD's is the pinned photodiode (PPD), shown in Fig. 4.9, which can significantly reduce dark current [15]. This photodiode has a p^+np^- structure where the two p regions are at the same potential as the substrate. The region of the diode that collects photons is buried beneath the surface so surface effects such as generation-recombination from the oxide-silicon interface are minimized. Increasing the bias on the n-region causes the depletion regions of the two diodes of this device to grow. A disadvantage of this method is that it has a small area for collecting photons which reduces quantum efficiency. In addition it is more difficult to manufacture, requiring CMOS process steps which are not standard.

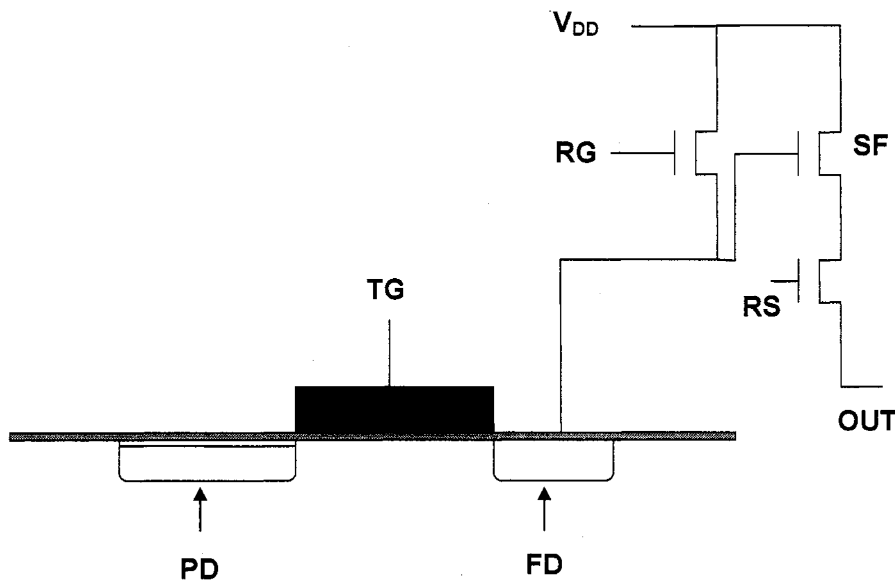

Fig. 4.9 Schematic of pinned photodiode [15].

4.6.5 Soft Reset

Recognizing the dominance of reset noise in low-light level imaging and the difficulty in implementing CDS, soft reset aims to reduce reset noise through the operation of the reset transistor. Soft reset is carried out by placing the same potential on the gate and drain of the NMOS reset transistor. With the gate and drain at the same potential, the transistor will be in weak inversion. In weak inversion, the current is of the form [2]

$$I = \exp\left[\frac{q\Delta V}{mkT}\right] \tag{23}$$

where $\Delta V = V_{GS} - V_{T,rst}$ and m is a non-ideality factor. Let F_n be the pdf that describes the probability that there are n electrons on the sense node at a point in time. Since drain-source voltage is much greater than the thermal voltage, current flows in one direction and we can describe how the number of electrons on the sense node changes with time [2]

$$\frac{\partial F_n}{\partial t} = F_{n-1} g_{n-1} - F_n g_n \tag{24}$$

where the probability of adding an electron to the sense node with n electrons already on the sense node is given by [2]

$$g_n \sim \exp[-\beta \cdot n] \tag{25}$$

where $\beta^2 = q^2/mkTC$. From (24), the change in variance with the average number of electrons on the sense node, $\hat{n}$, can be found [2]

$$\frac{d\sigma^2}{d\hat{n}} \approx 1 + 2\frac{dg}{dt}\frac{1}{g}\sigma^2 \tag{26}$$

The variance or reset noise can now be solved to get [2]

$$\sigma^2 = \frac{1}{2\beta}\left[1 - e^{-2\beta\Delta n} + 2\beta e^{-2\beta\Delta n}\sigma_o^2\right] \tag{27}$$

For the case of the photodiode active pixel sensor, this further reduces to [2]

$$\sigma^2 = mkTC/2 \qquad \text{for } \beta\cdot\Delta n >> 1 \tag{28}$$

and

$$\sigma^2 = \Delta n \qquad \text{for } \beta\cdot\Delta n << 1 \tag{29}$$

During reset, the sense node will charge up to a value which depends on the voltage on the sense node and the length of time of the reset. Therefore the reset voltage is not a predetermined value like in a hard reset operation. This leads to high image lag and low-light-level-non-linearity.

5 Reset Noise from a Mesoscopic Perspective

As the dominant source of noise, various attempts have been made to reduce the reset noise in the pixel as discussed in the previous chapter. CMOS technology has pushed towards increasingly smaller device dimensions. This impacts the reset noise where just even one electron added to the sense node can affect the sense node voltage. Consequently a study of reset noise and simulation from a mesoscopic perspective is appropriate.

By simulating soft reset, a simple means of reducing reset noise can be verified. Furthermore, the simulation can be used as a tool to further investigate soft reset and optimize it as a technique to reduce reset noise. Since a mesoscopic approach is being taken, the electron transport in the pixel was studied. Specifically, the movement of electrons from the channel of the reset transistor to the sense node capacitance that is formed by p-n junctions was simulated.

For the simulations, first a p-n diode corresponding to source to bulk p-n diode with a constant current source was simulated. This situation has been studied theoretically and reported in [16]. The authors found that sub-Poissonian shot noise and negligible thermal noise levels can be achieved depending on the junction capacitance and temperature. In addition, they found that as the capacitance decreases, an electron is thermionically emitted at regular intervals. This can be applied to the case of reset noise in a pixel which is dependent on the capacitance and temperature. Next using the same methodology, a p-n diode with a voltage-controlled current was simulated. The voltage controlled current was modeled after the current in a NMOS transistor in weak inversion. This is the case

found in the actual pixel where the voltage on the sense node changes the current in the junction. This chapter provides the background behind the theory and equations that were used in the simulations.

5.1 Thermionic Emission (TE) in a p-n diode

A single electron will be thermionically emitted at distinct intervals in time when the p-n junction voltage gets small enough that the single electron charging energy surpasses kT [16]. The thermionic emission rate, $K(t)$, is given by [16]:

$$K(t) = \frac{AT^2 A^*}{e} \exp\left[\frac{e}{kT}\left(V_j(t) - V_{bi} - \frac{e}{2C_{dep}}\right)\right] \tag{30}$$

where A is the area of the junction, A^* is the Richardson's constant, e is the charge of an electron, $V_j(t)$ is the junction voltage, and V_{bi} is the built-in potential. When an electron is thermionically emitted across the depletion layer the potential barrier increases and the depletion region width increases. The junction voltage affects the width of the n-depletion which changes the depletion layer capacitance which changes the effective potential barrier from the N to P.

5.2 Coulomb blockade effect

Consider a p-n junction with an external constant current source with a small junction capacitance as is commonly found in today's image sensors. In the last term of (30), there is an increase in the energy barrier. The V_{bi} is replaced by V_d, an effective built-in potential which is shown below:

$$K(t) = \frac{AT^2 A^*}{e} \exp\left[\frac{e}{kT}\left(V_j(t) - V_d\right)\right] \tag{31}$$

where

$$V_d = V_{bi} + \frac{e}{2C_{dep}} \tag{32}$$

This term, (32), is not present for macroscopic p-n junctions. If an electron has energy above this effective built-in potential, it may be thermionically emitted across the junction. This TE event decreases the junction voltage thereby reducing the chance of another TE event until the voltage, V_j, increases again due to the external constant current source. This is the coulomb blockade effect.

5.3 Operational Regimes

There are four regions of operation for a p-n diode driven by constant external current. They are the mesoscopic, sub-Poisson, Poisson, and macroscopic regimes. There are a few factors to consider when determining regime of operation. The first is r, the ratio between the electrostatic energy for a single electron and kT, where k is Boltzmann's constant and T is temperature, which is given by [16]

$$r = \frac{\left(q^2 / C_{dep}\right)}{kT} = \frac{e^2}{kTC_{dep}}. \tag{33}$$

Along with r, the observation time, T_{meas}, and the TE time constant, given by [16]

$$\tau_{te} = \frac{\tau}{r} \tag{34}$$

where $\tau = q/I$ is the single electron charging time, determine the operational regime.

5.3.1 Mesoscopic (Coulomb Blockade) Regime

If $r > 1$, then the electrostatic energy for a single electron is greater than *kT*, and the p-n diode is operating in the mesoscopic regime. In the mesoscopic regime, the junction voltage will increase and decrease at regular intervals and a graph of the junction voltage versus time will appear as a saw tooth pattern as shown in Fig. 5.1. This is due to the transport of an electron across the junction to the p-side or movement from p-side to n-side.

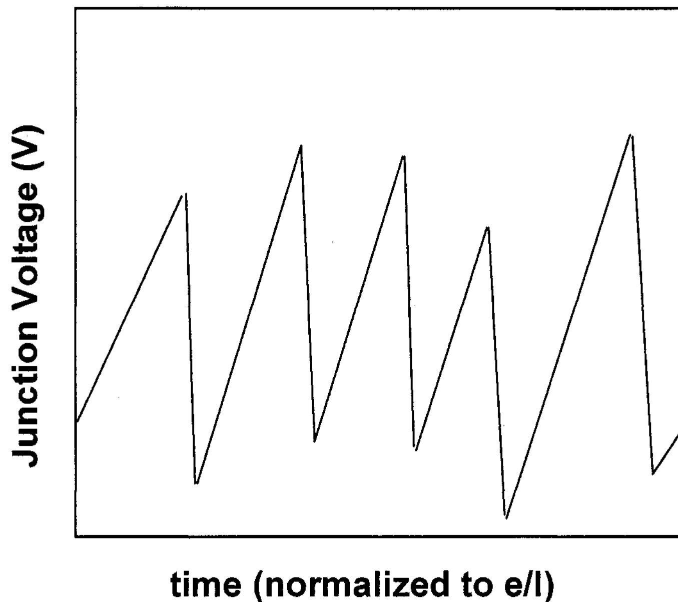

Fig. 5.1 Junction voltage vs. time for mesoscopic p-n junction with constant current source[17].

The junction is charged up steadily by the external constant current. This increases the probability of a TE event until a time interval of τ_{te} has elapsed since the last TE event. At this point, a TE event will occur and the junction voltage will decrease immediately and significantly, exhibiting the coulomb blockade effect. Capacitances in the attofarads are sufficient for operation in the mesoscopic regime.

5.3.2 Sub-Poisson Regime

A p-n diode is in the sub-Poisson regime when $r < 1$ and $T_{meas} > \tau_{te}$. This means that the electrostatic energy of an electron is less than kT and the observation time is less than the TE time constant. In this regime, the single electron coulomb blockade effect is not significant. Instead a number of electrons, n_e, collectively undergo a coulomb blockade effect. These electrons are charged continuously and are successively emitted, just as in the case of the single electron coulomb blockade effect. An example of this effect can be found as early as the 1920's in the sub-shot-noise of a space-charge-limited vacuum tube [18]. A p-n diode with a capacitance in the femtofarads range is an example of the sub-Poisson regime. Because of the small capacitance found in today imagers, this regime becomes their most important.

5.3.3 Poisson Regime

In this regime $r < 1$ and the time interval T is less than τ_{te}. This means that kT is greater than the electrostatic energy of an electron and the TE time constant is greater than a given time interval. The probability of n_e electrons emitted during T will have a Poisson distribution. An example of this is a p-n diode with a kTC value which is less than q^2. This can correspond to a p-n diode at room temperature with a large capacitance, much larger than the femtofarad range.

5.3.4 Macroscopic Regime

When $r << 1$ and the lifetime of an electron in the p-side, $\tau_n >> \tau$, the p-n diode is in the macroscopic regime. This is the case when kT is much larger than the electrostatic

energy of an electron and the electron lifetime in the p-side is much greater than the single electron charging time. The noise can be described by the long-known descriptions given in [11]. An example of a p-n junction in the macroscopic regime is one with a kTC value which is much less than q^2. This applies to a p-n diode at a high enough temperature and significantly greater than femtofarad capacitance.

5.4 Probability of Thermionic Emission

For reset noise, we are concerned about the fluctuations in the number of electrons on the sense node. So we must consider the number of electrons arriving and leaving from the sense node. Therefore the probability of a certain number of electrons being emitted from the sense node during an observation time will depend on the number of electrons on the node. For a p-n diode in the sub-Poisson regime let $\wp(k,t)$ represent the distribution of the number of electrons in a charge packet during a time interval of length t. Since this is a Gaussian process, it is given by [6]

$$\wp(k,t) = \frac{1}{\sqrt{2\pi\left(\sigma_{n_e}^2\right)}} \exp\left[-\frac{\left(n_e - \bar{n}_e\right)^2}{2\left(\sigma_{n_e}^2\right)}\right] \tag{35}$$

with a variance given by [6],

$$\sigma_{n_e}^2 = \frac{1}{r} = \frac{k_B T q^2}{C} \tag{36}$$

The probability of arrival of a charge packet at the source is Poisson and given by [6]

$$W(n) = \frac{(\lambda t)^k e^{-\lambda t}}{k!} \qquad t \geq 0, k = 1,2,\ldots. \tag{37}$$

with a variance given by [6]

$$\sigma_{n_e}^2 = \bar{n}_e \qquad (38)$$

where k_B is Boltzmann's constant.

Using the Burgess Variance Theorem, we can find the variance in the number of electrons thermionically emitted by multiplying (35) and (37). This leads to the probability of n_e electrons being emitted during a observation time interval T_{meas}, is given by [16]

$$P(n_e, T_{meas}) \simeq \frac{1}{N(r, \bar{n}_e)} \frac{1}{n_e!} \bar{n}_e^{n_e} \exp[-\bar{n}_e] \exp\left(-\frac{r}{2}(n_e - \bar{n}_e)^2\right) \qquad (39)$$

where $\bar{n}_e = T_{meas} I/e$ and $N(r, \bar{n}_e)$ is a normalization factor.

5.5 Collective vs. single electron coulomb blockade regime

There is a collective coulomb blockade regime and a single electron coulomb blockade regime. The collective coulomb blockade regime arises when $1/r$ is less than the number of electrons emitted in a time interval t. The last term in (39) dominates and the probability becomes Gaussian. So in this case, the variance of (39) given in (36) decreases linearly with $1/r$ and if expressed in terms of the number of electrons on the sense node is

$$n_e = \frac{C}{q}\sqrt{\frac{kTq^2}{C}} = \sqrt{kTC} \qquad (40)$$

which reduces to kTC.

Single electron coulomb blockade regime is when $1/r < 1$ (kT<single electron charging energy). The junction voltage fluctuates between a high and low value much

like that found in Fig. 5.1 as a single electron is thermionically emitted followed by the subsequent linear increase in junction voltage due to the constant current. For this case, the variance is suppressed to below an electron because only one electron is thermionically emitted due to the small capacitance.

6 Monte Carlo Simulation of Reset Noise

As been previously established, reset noise will play an increasingly important role in the performance of a CMOS image sensor as device dimensions shrink. The ability to simulate reset noise through the study of electron transport is of importance for its application to image sensors. It provides valuable insight into the factors affecting reset noise and can be used as a tool for further study and potential reduction of reset noise.

The complicated problem of electron transport in the pixel can be simplified with a numerical approach found in the Monte Carlo method. Solving equations analytically for hundreds or even thousands of electrons would be prohibitively difficult if not impossible. With Monte Carlo simulation, electron transport for hundreds and even thousands of electrons can be analyzed with available computing power in a straightforward way. Monte Carlo simulation uses probability density functions (pdfs) to define a physical system. A random number generator is used to generate uniformly distributed random numbers from 0 to 1. A rule to compare the randomly generated number will decide if an event has occurred. Finally the number of events is tracked and a variance is calculated.

The Monte Carlo method was used to first simulate thermionic emission in a silicon p-n diode then building on the p-n diode, reset noise was simulated for the pixel in the CMOS image sensor. It consists of simulating electrons arriving and leaving the diode which is described stochastically using given probabilities from known physical processes. The simulation starts with a description of the physical systems under study. These are defined by the system parameters and physical values characterizing the diode

and or transistor. In addition, parameters are chosen to control the simulation which can affect the accuracy of the results such as the number of time steps taken and the number of trials performed.

6.1 Monte Carlo simulation of p-n diode thermionic emission

A flow diagram demonstrating the algorithm used to simulate thermionic emission of a p-n diode under constant external current is shown in Fig. 6.1. The parameters describing the p-n diode are given in Table 2.

Table 2 Simulation parameters for pn diode.

Temperature, T	300 K
Donor concentration, ND	10^{15} cm^{-3}
Acceptor concentration, NA	10^{17} cm^{-3}
Capacitance, C	1 fF
Series resistance, R_S	3 kΩ

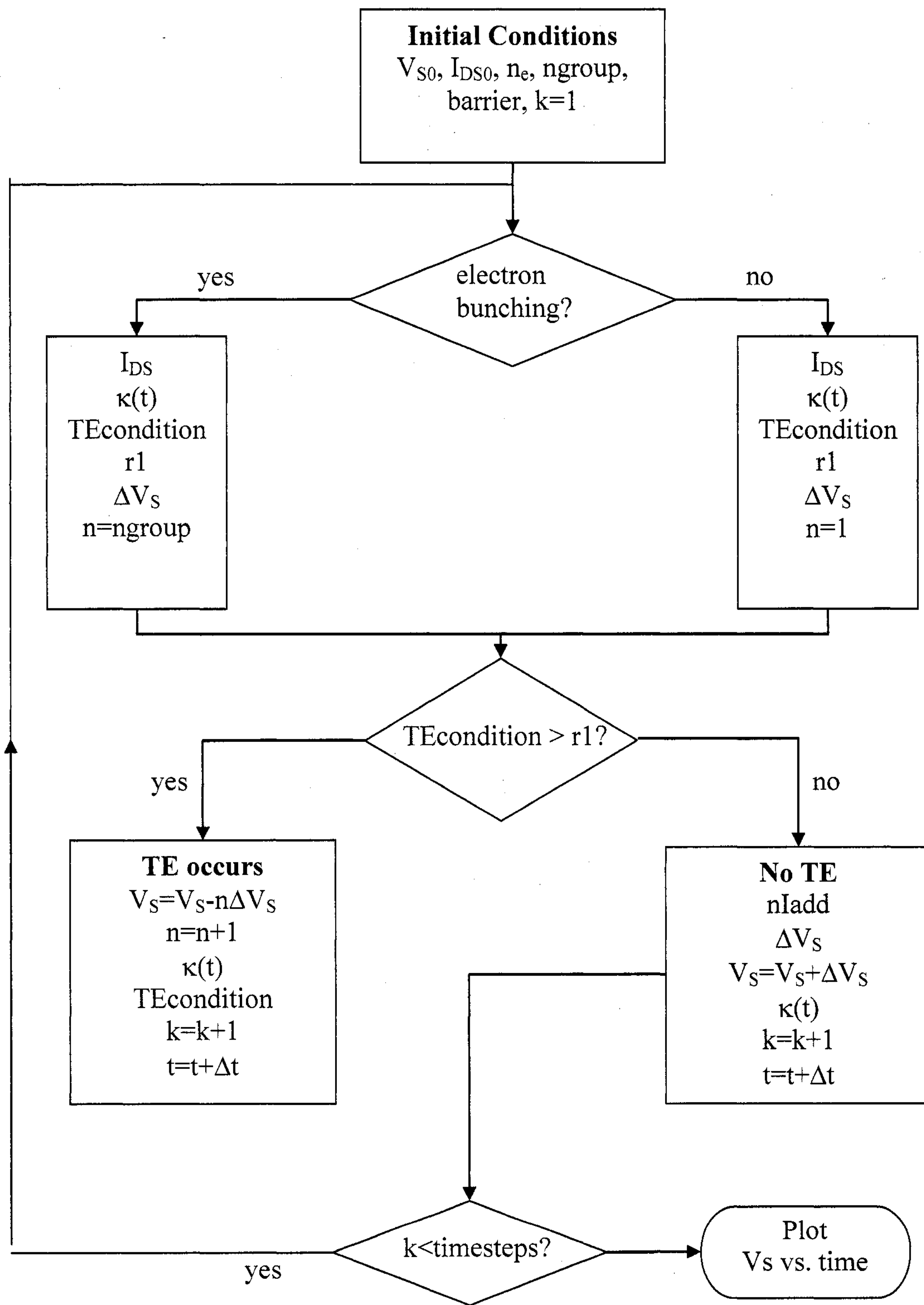

Fig. 6.1 Algorithm used in simulation thermionic emission in pn diode.

The simulation starts at time, $t=0$. Based on the current, the initial junction voltage is calculated along with the barrier. Two cases were simulated. The first was with a constant current. The second was with a voltage dependent current. The matlab script TEpnconsI.m was used for the constant current case and the matlab script TEpn.m was used for the voltage controlled current case. Both scripts can be found in the appendix. The voltage controlled current, I_{DS}, used a weak inversion source-referenced model given by [19]

$$I_{DS} = \frac{W}{L} I'_M e^{(V_{GS}-V_M)/(n\phi_t)} (1 - e^{-V_{DS}/\phi_t}) \tag{41}$$

where

$$V_M = V_{FB} + 2\phi_F + \gamma\sqrt{2\phi_F + V'_{SB}} \tag{42}$$

and

$$I'_M = \mu \frac{\sqrt{2q\varepsilon_S N_A}}{2\sqrt{2\phi_F + V'_{SB}}} \phi_t^2 \tag{43}$$

and

$$n = 1 + \frac{\gamma}{2\sqrt{2\phi_F + V'_{SB}}} \tag{44}$$

where W and L are the transistor's dimensions, V_{GS} is the gate-source voltage, φ_t is thermal voltage, V_{FB} is flatband voltage, is φ_f fermi level, q is electron charge, ε_s is silicon permittivity, and γ is body effect coefficient. The parameters for this transistor are shown in Table 3.

Table 3 Simulation parameters used for voltage controlled current.

Channel width, W	100 μm
Channel length, L	5 μm
Donor concentration, ND	10^{15} cm^{-3}
Acceptor concentration, NA	10^{17} cm^{-3}
Oxide thickness, t_{ox}	100A
Capacitance, C	1 fF

The step size (ΔT), measurement time interval (T_{meas}), and number of time steps (k) to run the Monte Carlo simulation is chosen, based on the value of the junction capacitance. If the junction capacitance is large enough so that the following equation is satisfied,

$$\frac{q}{C} < \frac{kT}{q} \tag{45}$$

electrons will be thermionically emitted in groups of electrons. If the opposite is true, individual electrons will be emitted. If the thermal voltage is greater than the change in junction voltage due to thermionic emission, then electrons will be thermionically emitted in groups. The number of electrons in each group will be Gaussian distributed with mean, $\overline{n_e}$, given by [16]

$$\overline{n_e} = T_{meas}\frac{I}{e} \tag{46}$$

where T_{meas} is the measurement time, I is the current, and e is electron charge. It will have a standard deviation given by [16]

$$\sigma = \frac{1}{\sqrt{r}} \tag{47}$$

Using the mean and standard deviation, the number of electrons that will be thermionically emitted is randomly selected.

After the initial values for junction voltage and barrier are calculated, a time step is taken and $K(t)$, the thermionic emission rate, is calculated using (30). A uniformly distributed random number between 0 and 1 is chosen for $K(t)$. If $r1<K^*\Delta T$, then thermionic emission has occurred and the junction voltage drops by $n^*(q/C)$ where n is the number of electrons thermionically emitted, q is electron charge, and C is the diode capacitance. n is chosen from a Gaussian distribution with mean given by [16]

$$\overline{n}_e = T_{meas} \frac{I}{e} \tag{48}$$

and variance of $2/r$. The simulation then advances a time step. Otherwise the junction voltage is increased depending on the current's value. This is repeated until the predetermined number of time steps have been taken. After this time has been reached, the highest voltage from time=0 to the end of the measurement time is recorded. . A sample plot of the p-n diode's voltage vs. time for a constant current is shown in Fig. 6.2. Fig. 6.3 gives the same plot but with a voltage dependent current as is found in an actual pixel.

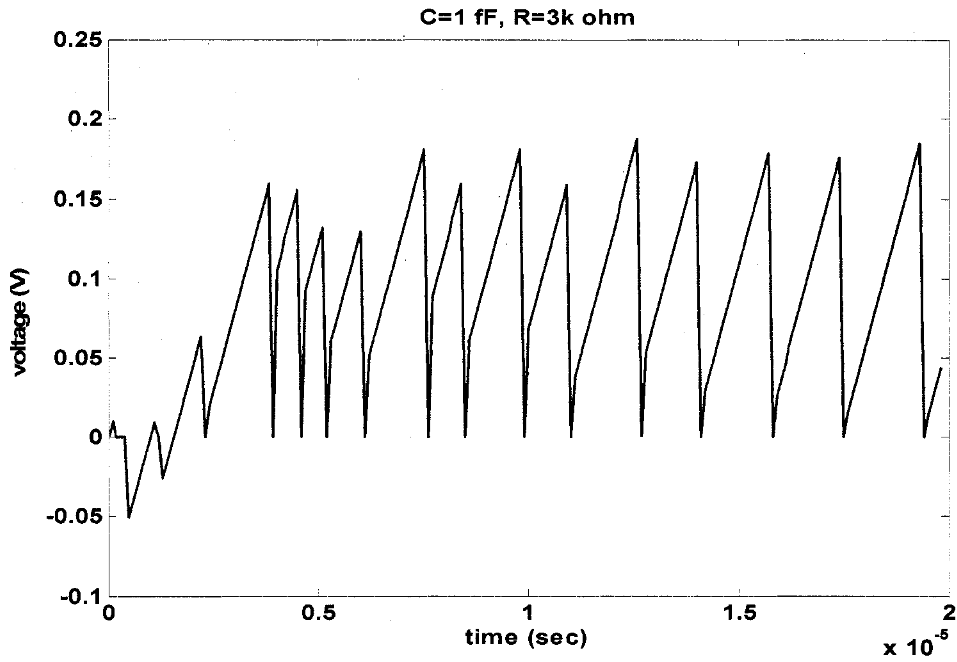

Fig. 6.2 Simulated junction voltage vs. time for thermionic emission in a p-n diode with constant current.

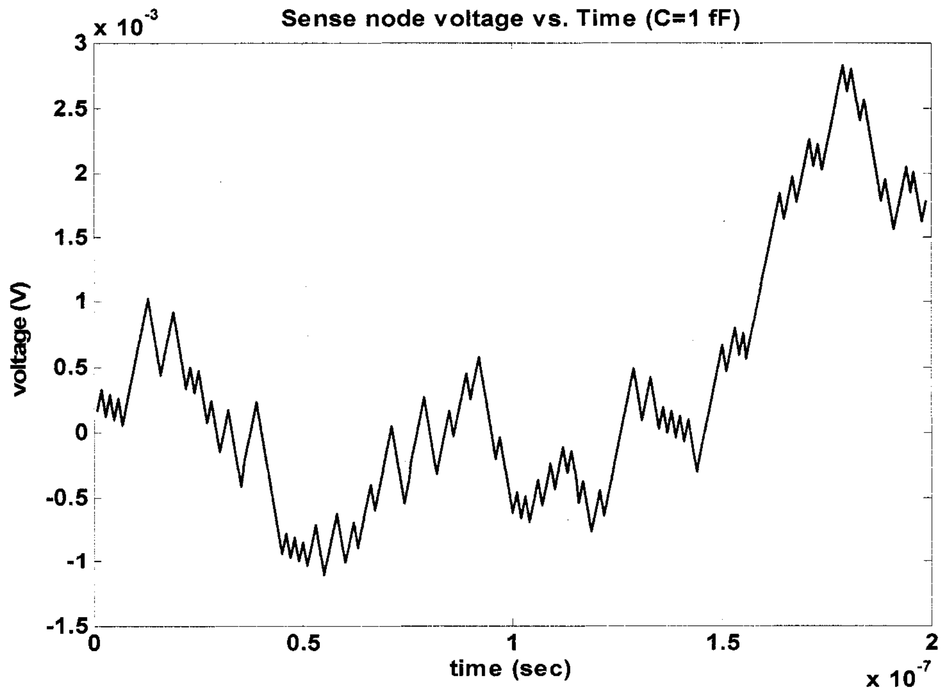

Fig. 6.3 Simulated junction voltage vs. time for thermionic emission in p-n diode with voltage dependent current.

6.2 Monte Carlo simulation of reset noise in CMOS image sensor pixel

Reset noise is determined from the simulation by recording the highest voltage in each trial of the thermionic emission in the p-n diode with a voltage dependent current. In this case, the simulation was repeated for 1000 trials. The algorithm is illustrated in the flow chart found in Fig. 6.4. The standard deviation of these highest voltages gives the value for the simulated reset noise. Fig. 6.5 shows a histogram of the highest sense node voltages. This represents the distribution of reset noise which is Poissonian. The simulated reset noise voltages are shown in Fig. 6.6. Fig. 6.7 is a histogram of the highest sense node voltages which has a Gaussian shape for soft reset. Fig. 6.8 is a plot of the highest sense node voltages vs. time for soft reset.

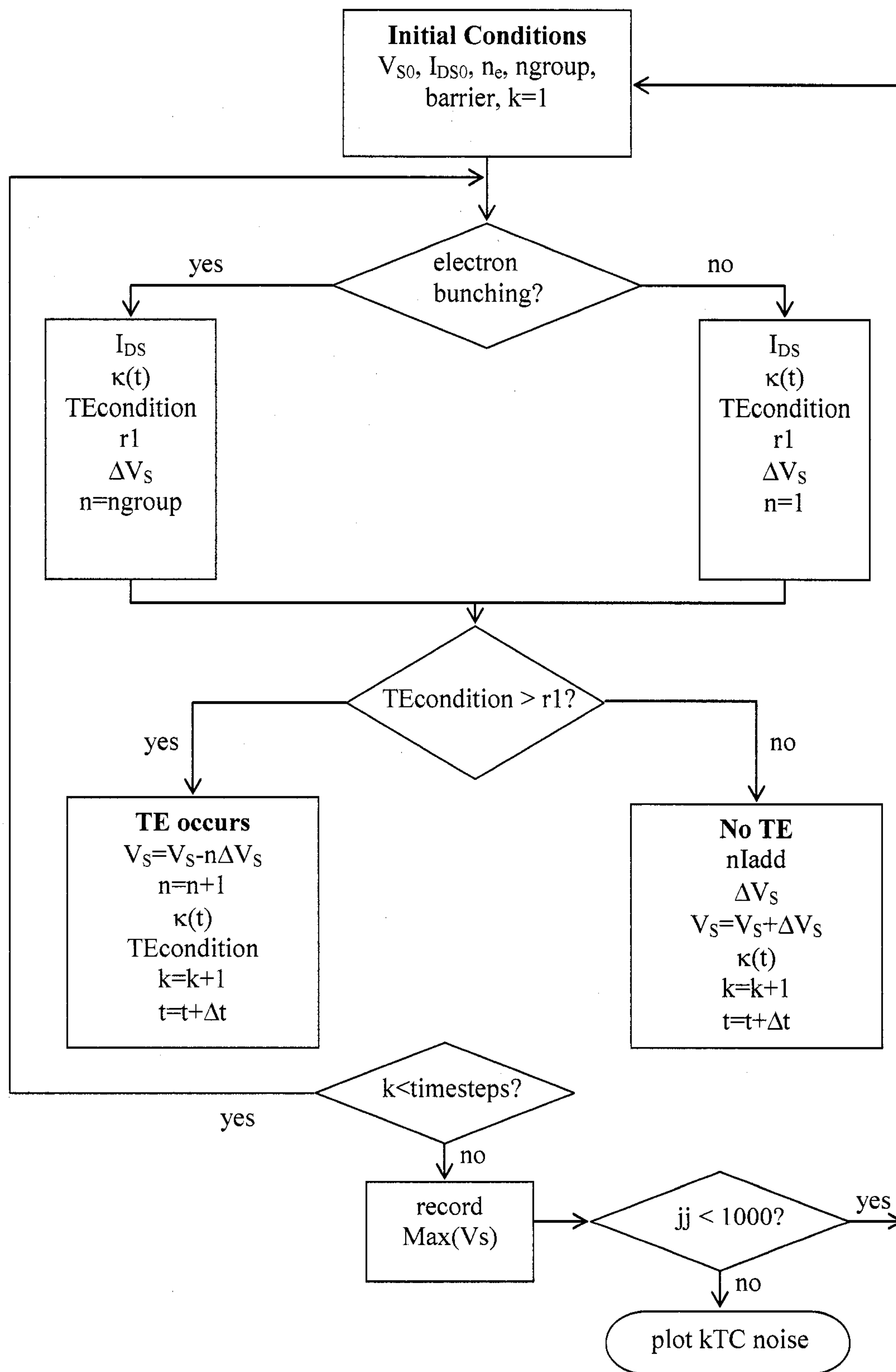

Fig. 6.4 Algorithm used to simulate reset noise in CMOS image sensor pixel.

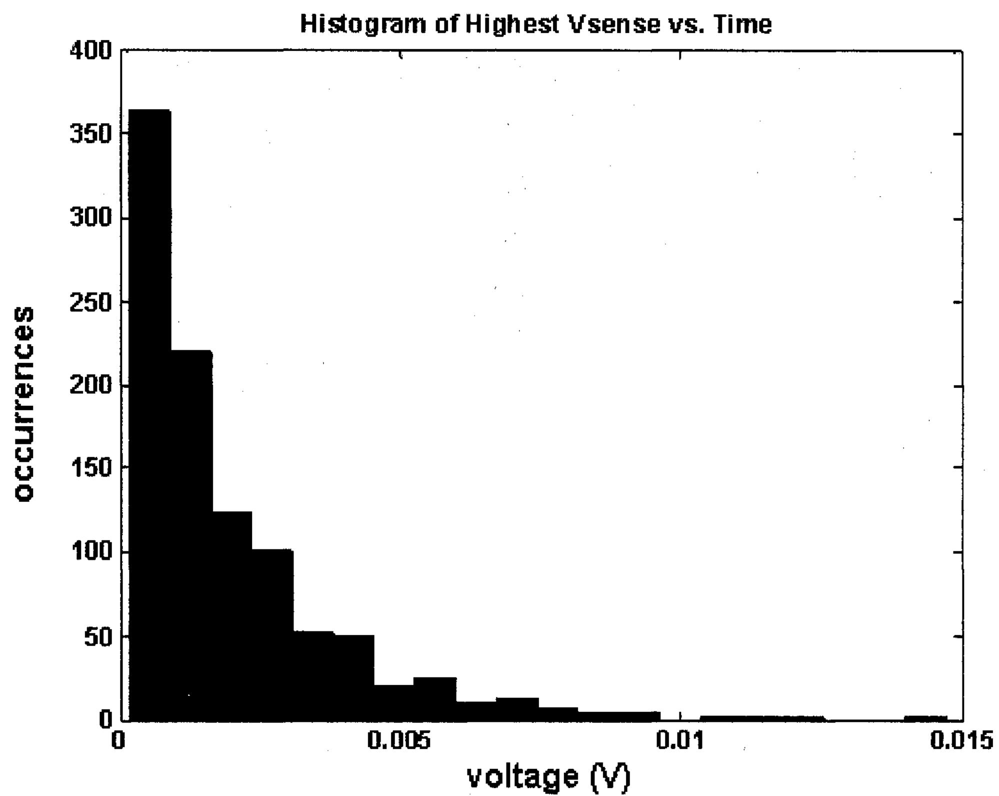

Fig. 6.5 Histogram of conventional reset noise in CMOS image sensor pixel.

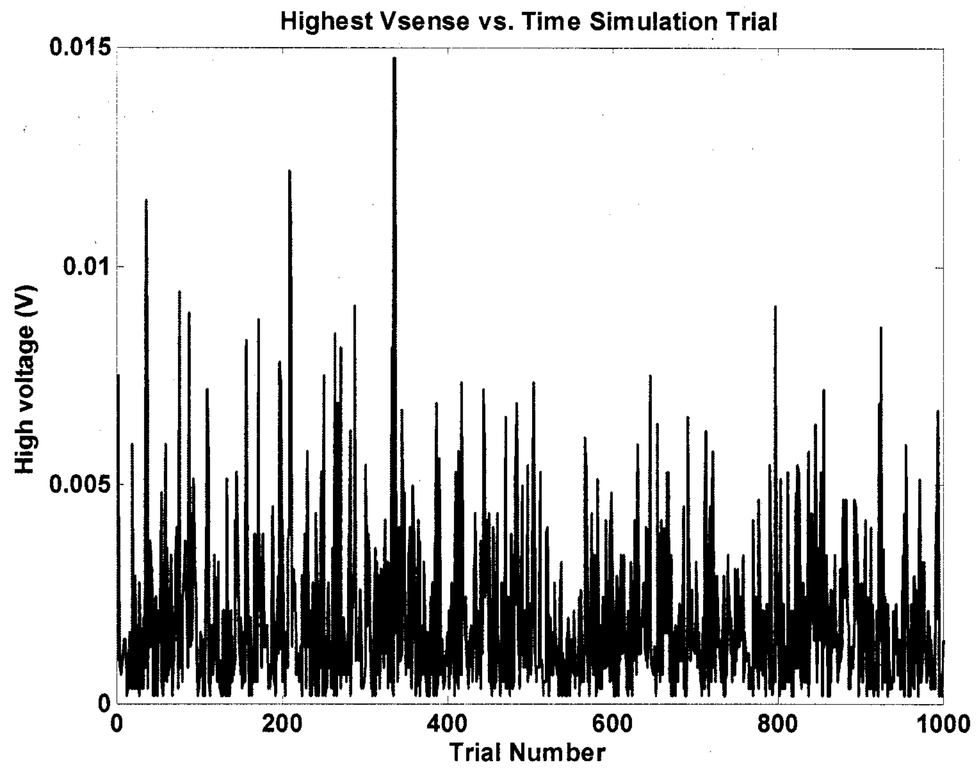

Fig. 6.6 Simulation of conventional reset noise in CMOS image sensor pixel.

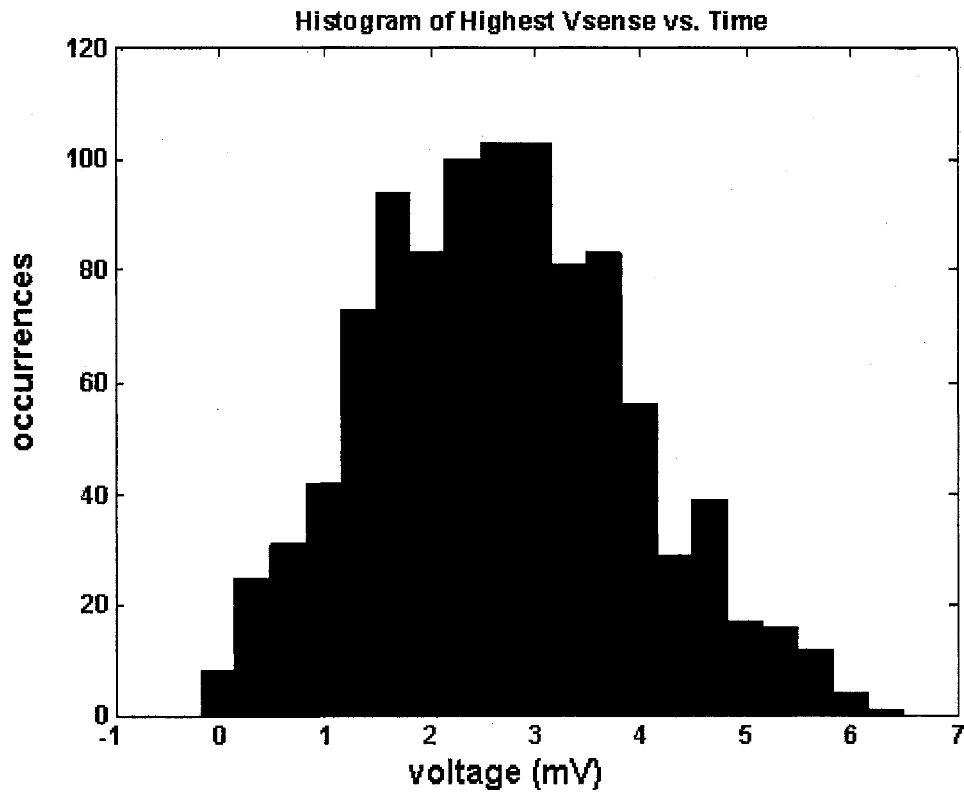

Fig. 6.7 Histogram of highest sense node voltages for soft reset.

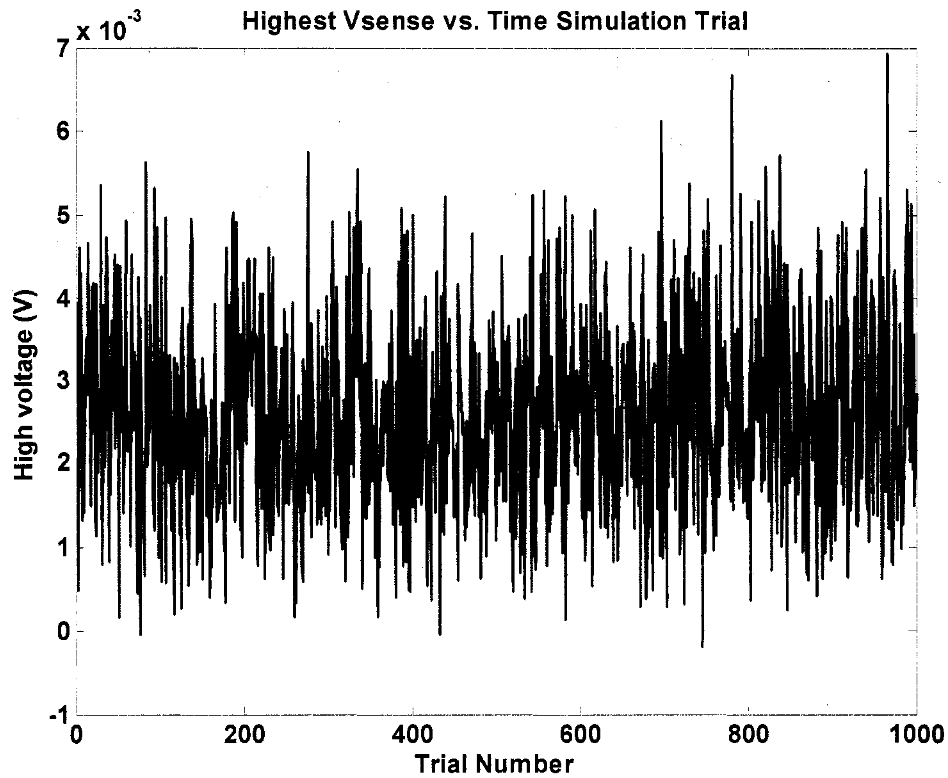

Fig. 6.8 Simulated highest sense node voltage vs. time in CMOS image sensor pixel for soft reset.

6.3 Results and Discussion

The simulation for p-n diode thermionic emission under constant current shows that mesoscopically, the thermionic emission events are regulated. A coulomb blockade effect similar to that presented in [16], was observed in simulation for a silicon p-n diode with constant current at room temperature.

However, if the current is no longer constant but is voltage dependent, the saw-tooth oscillations typifying a coulomb blockade effect is not seen. Just after thermionic emission, a subsequent thermionic emission event is suppressed due to a voltage drop which is determined by the diode's capacitance. The junction voltage must increase to its

previous value before another thermionic emission event may occur. In the constant current case, electrons are being added at a constant rate so the time it takes to regain that voltage will be consistent between thermionic emission events. This gives Fig. 6.2 its periodic waveform pattern and Fig. 6.3 its random waveform pattern.

In the simulation for thermionic emission in a p-n diode under a voltage dependent current, the waveform lacks this periodic saw-tooth pattern. Unlike the constant current case, the current changes each time step so it can not be predetermined when the junction voltage will be sufficient for thermionic emission. These times will occur randomly. Since electrons are leaving the node in groups of electrons, the highest voltage where thermionic emission occurs will also vary unlike the constant current case.

For a conventional reset, the simulated value of 0.0019V closely matches the calculated value of 0.002V. This comes out to a 6% difference between the simulation and expected value. In a conventional reset, the reset transistor will turn on by putting a voltage greater than the threshold voltage on the gate. Therefore the sense node voltage may change greatly by electrons arriving and leaving the sense node. The reset transistor can not prevent the electrons from behaving this way.

The p-n diode simulation with voltage dependent current is the situation found in a CMOS image sensor pixel where a photodiode is connected to a reset transistor. Since the voltage controlled current is represented by a weak inversion source reference model, it applies directly to soft reset. In soft reset the gate and drain voltage are at the same potential, therefore the transistor is operated in weak inversion.

The output statistics from the soft reset simulation produced simulated reset noise of 0.0012 V. The calculated reset noise is 0.0020 V. This is a 40% reduction in reset noise from using soft reset. This improvement comes from the introduction of a feedback mechanism from the reset transistor being in weak inversion during reset operation. For weak inversion, the current increases exponentially with the voltage difference between the gate-source voltage and the threshold voltage. An increase in the sense node voltage causes the current flow to quickly decrease. This decreases the variance in the sense node voltage resulting in lower reset noise. This matches the work done by B. Pain et al. in [2] where a square root of two reduction of reset noise was predicted for the ideal case.

7 Conclusion

Reset noise places a limitation on the performance of a CMOS image sensor. It is the dominant source of noise in the imager especially for low-light level conditions. The need for mobile devices requires increasingly smaller imagers. It is at these small device sizes that reset noise affects the imager the most due the small capacitances associated with the pixel.

In this thesis, the reset noise in a CMOS image sensor pixel and different techniques to reduce it was studied. Monte Carlo simulation of the reset noise in the imager and soft reset as a means to reduce reset noise was performed using Matlab. The simulated reset noise agreed with the expected value. Using this simulation as a platform to simulate soft reset in the pixel, this approach was found to reduce the reset noise by 40% which agrees with work done by B. Pain et al. in [2].

7.1 Future Work

This thesis looked at reset noise from the ideal case. More sophisticated models of thermionic emission rate, current, and reset transistor could be used where the non-ideal case is considered. Future work could include changing various parameters of the reset transistor and discovering their effect on the reset noise. The reset transistor can be biased in different ways to see their effect on reset noise. The measurement time and the thermionic emission times can be altered to see how this changes the reset noise. The temperature can be varied to see its effect on reset noise as well.

Appendix A: MATLAB® Code

The version of MATLAB® used for all simulations was Matlab6.5r13.

TEpnconsI.m

```
% Filename: TEpnconsI.m
% Written by: Irene Calizo Feb 2005
% Last Revised: 03-June-2005 night
% San Jose State University
%
% REQUIREMENTS:
%
% Toolboxes: Statistics
% Other m-files: none
% Other files: none
% Functions:  none
% Subfunctions: None
%
% This script performs a Monte Carlo simulation for TE of a p-n diode
% ---------------------------------------------------------------------

clear all;

% **** CONSTANTS *** %
% Planck's Constant (eV*s)
h = 4.14*10^-15;
% Thermal voltage (at 300K)
kToverq=0.0259; % (V)
kT = 0.026; % (eV)
% Boltzmann's constant
kB=1.38e-23;
% electron charge (C)
q = 1.6*10^(-19);
e = 1.6*10^(-19);
% electron mobility in Si (cm^2 / V*s)
%un=1450;
% Effective density of states in the conduction band for Silicon
Nc=2.86*10^19;
% Intrinsic carrier concentration (cm-3)
ni = 9.65*10^9;
% Permittivity in vacuum (F/cm)
```

```
epsilonNot=8.85*10^-14;
% Dielectric constant of Silicon
kSi=11.9;
% Silicon permittivity (F/cm)
epsilonSi=kSi*epsilonNot;

% Impurity doping concentrations(cm-3)
ND = 10^17;
NA = 10^15;
% Band digram info
Ec_2_Ef=kT*log(Nc/ND);
Ef_2_Ei=kT*log(ND/ni);
% Ei = 0;
Ef=Ef_2_Ei;
Ec=Ef+Ec_2_Ef;
% Changing these values
Cdep=1e-15; % farads
Rs=3e3;
% Built in potential (eV)
Vbi=kT*log( (ND*NA)/ni^2 ) + Ef;  % This is relative to Ei so must add Ef
% Effective built-in potential (eV)
Vd=Vbi+(e^2/(2*Cdep));
% Free electron mass from cover of Yang (kg)
m=9.1e-31;
% electron effective mass for Si from Yang
me=0.22*m;
%%%%%%%%%%%%%%%%%%%%%%end
constants%%%%%%%%%%%%%%%%%%%%%%%%

t=0; % initialize time
% p-region x-sectional area
A=1;
% external continuous circuit current (A)
I=1e-10; % just testing
% Number of time steps to take for jcn voltage vs. time plot
timeSteps=200;
%%%%%%%%%%%%%%%%%%%%%%%%
% Maximum number of electrons TE'd for a given constant current per second
nmax=I/q;
% Recombination Time (sec)
Trecomb=7E-20;
% Effective cross-sectional area of n-type layer (cm^2)
Aeff=1;
% Room Temperature (K)
```

```
T=300;
% Richardson's constant (A/K^2-cm^2) for n and p-type Silicon
Astarrn=110;
Astarrp=32;
% Time Step (sec)
deltaT=1e-7;
% parameter for the ratio of single-electron charging energy and the
%   characteristic energy of thermal fluctuation
r = ((q^2)/(Cdep*kB*T))
% single electron charging time aka tau
tau = q/I;
% single electron charging time aka tau
elechargtime = q/I;
t=elechargtime;
Tmeas=1e-6;
% Max number of electrons can get from current per unit time
nmax=Tmeas*I/q;
% average number of electrons that are TEd
nebar=nmax*(deltaT/Tmeas);
% make t less than tauTE, Ktime is t in the K(t) eqn in the paper
Ktime=deltaT; % should be equal to deltaT
% thermionic emission time aka tauTE
TEtime = elechargtime/r
timeInt=1e-15; % time used to determine how many electrons go collectively
%%%%%%%%%%%%%%%%%%%%%%%%
  Vjo=I*Rs; % initial junction voltage due to external current (V).
  Vj=Vjo; % for first time step, Vj=Vjo
  noft=0;
  n=1; % initial number of electrons
  barrier=Vd-Vj; % barrier to TE
  ngroup=1; % group of electrons jump barrier, initialize to 1 so no divide by zero warning
  groupind=0; % 1 means a group of electrons is waiting to TE, 0 is normal
  k = 1; % index for time, so can of limit no. of time steps which is the Tmeas
  nind=1; % index for checking ngroup
  neTE=0; % total number of electrons TE'd

Vjo=I*Rs; % initial junction voltage due to external current (V).
  Vj=Vjo; % for first time step, Vj=Vjo
  noft=0;
  n=1; % initial number of electrons
  barrier=Vd-Vj; % barrier to TE
  ngroup=1; % group of electrons jump barrier, initialize to 1 so no divide by zero warning
  groupind=0; % 1 means a group of electrons is waiting to TE, 0 is normal
  k = 1; % index for time, so can of limit no. of time steps which is the Tmeas
```

```
   nind=1; % index for checking ngroup
   neTE=0; % total number of electrons TE'd

% % determine if there is bunching
if ( (q/Cdep) < (kB*T/q) ) % q/Cdep is change in jcn voltage from TE,a kT/q is thermal voltage
   bunching = 1;
   nTE=ngroup; % number of electrons last TE'd
else
   bunching = 0;
end

if bunching==1  % bunching occurs, calculate TE the using Poisson & Gaussian

Kzero=((Aeff*T^2*Astarrn)/e)*exp((e/(kB*T))*(Vj-Vd)); % TE rate with no electrons TE'd yet
Koft=Kzero;
nTE=1; % so no divide by zero warning in K(t) expression
   while k <  timeSteps
            % decides whether TE will occur



            Koft=(Aeff*T^2*Astarrn/e)*(exp((e/(kB*T))*(Vj-Vd)));
            if (nTE == 0)
               Kexpoft=exp((-r*n));
            else
               Kexpoft=(exp(((deltaT*Koft)/nTE)-(r*n)));
            end
            Koft=Kzero*Kexpoft; % TE rate (prob. of TE)
            TEcondition=Koft*deltaT;
            r1=unifrnd(0,1);  % used to compare to TEcondition to decide if TE occured.
            deltaVj=q/Cdep; % change in voltage from gaining or losing one electron
            r2=unifrnd(0,1); % used to compare to RecombCondition to decide if recombination
occured.

            % decides how many electrons will TE
            mean=nebar;
            sigma=sqrt(2/r);
            ngroup=randn*sigma+mean;
            ngroup=fix(ngroup); % rounds ngroup to an integer toward zero
            checkngroup(k,:)=ngroup;
            lambda=1; % on average in one time step, one electron will TE

            if (TEcondition > r1) % TE will occur
               Vj=Vj-(n*deltaVj); % group of e-s go so drop jcn voltage
```

```
            n=n+ngroup;
            Koft=(Aeff*T^2*Astarrn/e)*(exp((e/(kB*T))*(Vj-Vd)));
            if (nTE == 0)
              Kexpoft=exp((-r*n));
            else
              Kexpoft=(exp(((deltaT*Koft)/nTE)-(r*n)));
            end
            Koft=Kzero*Kexpoft; % TE rate (prob. of TE)
            TEcondition=Koft*deltaT;
            time(k,:) = t; % array of all time steps (s)
            t=t+deltaT; % go to next time
            k=k+1; % increments the time step
            nTE=ngroup; % for next loop, the number of elec. last TE'd
          else % no TE occurs
            nIadd=6.24e18*deltaT*I; % number of electrons to add from the current when no TE
occurs
            nIadd=round(nIadd); % rounds nIadd to nearest integer (can't have part of an electron)
            deltaVj=nIadd*q/Cdep; % change in junction voltage due to the current
            Vj=Vj+deltaVj; % increase junction voltage since no TE
            my_voltage(k,:)=Vj; % voltage for this time step
            Koft=(Aeff*T^2*Astarrn/e)*(exp((e/(kB*T))*(Vj-Vd)));
            if (nTE == 0)
              Kexpoft=exp((-r*n));
            else
              Kexpoft=(exp(((deltaT*Koft)/nTE)-(r*n)));
            end
            Koft=Kzero*Kexpoft; %TE rate (prob. of TE)
            checkn(k,:)=n; % for debugging
            time(k,:) = t;
            t = t + deltaT; % go to next time step
            k=k+1;
          end
            % check different variables for debugging.
      checkTEcondition(k,:)=TEcondition; % for debugging TE condition
      checkKoft(k,:)=Koft; % for debugging TE condition
      checkr1(k,:)=r1; % for debugging TE condition
      checkr2(k,:)=r1; % for debugging TE condition
      checkTEif(k,:)=(TEcondition)-r1; % for debugging TE condition
        end % end of while loop for bunching
      end % end of if bunching==1 statement

if bunching==0 % bunching doesn't occur, calculate TE the old way
          % doesn't usually go this way
  while k <  timeSteps
```

```
        % decides whether TE will occur
        Koft=(Aeff*T^2*Astarrn/e)*(exp((e/(kB*T))*(Vj-Vd)));
        Kexpoft=(exp(((deltaT*Koft)/nTE)-(r*n)));
        Koft=Kzero*Kexpoft; % TE rate (prob. of TE)
        TEcondition=Koft*deltaT;
        r1=unifrnd(0,1);  % used to compare to TEcondition to decide if TE occured.
        deltaVj=q/Cdep; % change in voltage from gaining or losing one electron
        TEconditionzero=Koftnzero*deltaT;
        r2=unifrnd(0,1); % used to compare to RecombCondition to decide if recombination
occured.
  if (TEcondition > r1) % TE will occur
        Vj=Vj-deltaVj; % group of e-s go so drop jcn voltage
        Koft=(Aeff*T^2*Astarrn/e)*(exp((e/(kB*T))*(Vj-Vd)));
        Kexpoft=(exp((deltaT/tauTE)-(r*n)));
        Koft=Kzero*Kexpoft; % TE rate (prob. of TE)
        TEcondition=Koft*deltaT;
        time(k,:) = t; % array of all time steps (s)
        t=t+deltaT; % go to next time
        k=k+1; % increments the time step
        n=n+1; % add another electron to TE current
        nTE=1; % for next loop, the number of electrons last TE'd
  else % no TE occurs
        nIadd=6.24e18*deltaT*I; % voltage from no. of electrons to add from the current when no
TE occurs
        deltaVj=nIadd*q/Cdep; % change in junction voltage due to the current
        Vj=Vj+deltaVj; % increase junction voltage since no TE
        my_voltage(k,:)=Vj; % voltage for this time step
        Koft=(Aeff*T^2*Astarrn/e)*(exp((e/(kB*T))*(Vj-Vd)));
        Kexpoft=(exp((deltaT/tauTE)-(r*n)));
        Koft=Kzero*Kexpoft; % TE rate (prob. of TE)
        checkn(k,:)=n; % for debugging
        time(k,:) = t;
        t = t + deltaT; % go to next time step
        k=k+1;
  end
  % check different variables for debugging.
  checkTEcondition(k,:)=TEcondition; % for debugging TE condition
  checkKoft(k,:)=Koft; % for debugging TE condition
  checkr1(k,:)=r1; % for debugging TE condition
  checkTEif(k,:)=(TEcondition)-r1; % for debugging TE condition
  end % end of while loop for no bunching
end % end of if bunching==0 statement

%%%%%%%%%%%%%%%%%%%%%%%%%%%%%%%%%%%%%%%%%%%%%%
```

```
%%%%%%%%%%%%%%%%%%%%%%%%%%%%%%%%%%%%%%%%%%%%%%%%
% plot the data

figure(1);
plot(time,my_voltage);
xlabel('time (sec)');
ylabel('voltage (V)');
title('C=1 fF, R=3k ohm');

figure(2);
hist(checkngroup,20);
xlabel('ngroup value');
ylabel('Number of Occurences')
title('Histogram of ngroup');
```

TEpn.m

```
% Filename: TEpn.m
% Written by: Irene Calizo Feb 2005
% Last Revised: 19-June-2005 night
% San Jose State University
%
% REQUIREMENTS:
%
% Toolboxes: Statistics
% Other m-files: none
% Other files: none
% Functions:  none
% Subfunctions: None
%
% This script performs a Monte Carlo simulation for thermionic emission in
% pn diode plotting junction voltage vs. time.

clear all;

% **** CONSTANTS *** %
% Planck's Constant (eV*s)
h = 4.14*10^-15;
% Thermal voltage (at 300K)
kToverq=0.0259; % (V)
phiT=kToverq;
kT = 0.026; % (eV)
% Boltzmann's constant
kB=1.38e-23;
% electron charge (C)
q = 1.6*10^(-19);
e = 1.6*10^(-19);
% electron mobility in Si (cm^2 / V*s)
%un=1450;
% Effective density of states in the conduction band for Silicon
Nc=2.86*10^19;
% Intrinsic carrier concentration (cm-3)
ni = 9.65*10^9;
% Dielectric constant of Silicon
kSi=11.9;
% dielectric constant of oxide
kox=3.9;
% Permittivity in vacuum (F/cm)
epsilonNot=8.85*10^-14;
```

```
% Oxide permittivity
epsilonox=kox*epsilonNot ;
% Silicon permittivity (F/cm)
epsilonSi=kSi*epsilonNot;
nuN=1450; % cm^2/V*S

% Transistor sizing (cm)
W=1e-2 ; % 100 um
L= 5e-4; % 5 um
% Impurity doping concentrations(cm-3)
ND = 10^15;
NA = 10^17;
tox=1e-6; % 100 angstroms=10nm=1e-6cm
% Band digram info
Ec_2_Ef=kT*log(Nc/ND);
Ef_2_Ei=kT*log(ND/ni);
% Ei = 0;
Ef=Ef_2_Ei;
Ec=Ef+Ec_2_Ef;
Coxprime=epsilonox/tox; % oxide cap. per unit area
% interface charge (C/cm2)
Qnotprime=1e-8;
phiMS=-Ef-0.56;
VFB= phiMS-(Qnotprime/Coxprime);
% Capacitance
Cdep=1e-15; % farads
% Resistance
Rs=3e3;
% Built in potential (eV)
Vbi=kT*log( (ND*NA)/ni^2 ) + Ef;  % This is relative to Ei so must add Ef
% Effective built-in potential (eV)
Vd=Vbi+(e^2/(2*Cdep));
% Free electron mass from cover of Yang (kg)
m=9.1e-31;
% electron effective mass for Si from Yang
me=0.22*m;
%%%%%%%%%%%%%%%%%%%%%%%%end
constants%%%%%%%%%%%%%%%%%%%%%%%%%%

t=0; % initialize time
% p-region x-sectional area
A=1;

% Number of time steps to take for jcn voltage vs. time plot
```

```
timeSteps=200;


%%%%%%%%%%%%%%%%%%%%%%%%%
% Recombination Time (sec)
Trecomb=7E-20;
% Effective cross-sectional area of n-type layer (cm^2) (made up)
Aeff=1;
% Room Temperature (K)
T=300;
% Richardson's constant (A/K^2-cm^2) for n and p-type Silicon
Astarrn=110;
Astarrp=32;
% Time Step (sec)
deltaT=1e-9;
% parameter for the ratio of single-electron charging energy and the
%   characteristic energy of thermal fluctuation
r = ((q^2)/(Cdep*kB*T));
bodyfactor=5.8e-16*sqrt(NA)/Coxprime ; % body effect coefficient
VSBprime=1; % fixed source body voltage
% Source voltage
VS=0; % start off with 0V
% Gate voltage
VG=0.1;
% Drain voltage
VD=0.3;
VGS=VG-VS; % gate source voltage
VDS=VD-VS ; % drain source voltage
VM=VFB+2*Ef+(bodyfactor*sqrt((2*Ef)+VSBprime)); % upper limit of W.I.
IMprime=nuN*((sqrt(2*q*epsilonSi*NA))/(2*sqrt(2*Ef+VSBprime)))*phiT^2;
n=1+(bodyfactor/(2*sqrt(2*Ef+VSBprime)));
% calculate voltage dependent current
IDS=(W/L)*(IMprime)*(exp((VGS-VM)/(n*phiT)))*(1-exp(-VDS/phiT)); % p. 173
IDSo=IDS; % initial current value with VS=0V

% single electron charging time aka tau
tau = q/IDS;

% single electron charging time aka tau
elechargtime = q/IDS;
t=elechargtime;
% time used to determine how many electrons go collectively
Tmeas=1e-6; %
% Max number of electrons can get from current per unit time
```

```
nmax=Tmeas*IDS/q;
% average number of electrons that are TEd
nebar=Tmeas*(IDS/q);
% make t less than tauTE, Ktime is t in the K(t) eqn in the paper
Ktime=deltaT; % should be equal to deltaT
% thermionic emission time aka tauTE
TEtime = elechargtime/r;
timeInt=1e-15; % time used to determine how many electrons go collectively
numTimesTE=0; % the number of times TE occurs
%%%%%%%%%%%%%%%%%%%%%%%%%%%%%%%%%%%%%%%%%%%%%%%%%%%%%%%%%%%%%%%%%%%%%%%%%%%%%%%%
%%%%%%%%%%%%%%%%%%%%%%%%%%%%%%%%%%%%%%%%%%%%%%%%

VSo=IDSo*Rs; % initial junction voltage due to external current (V).
  VS=VSo; % for first time step, Vjcn=Vjo
  noft=0;
  n=1; % initial number of electrons
  barrier=Vd-VS; % barrier to TE
  ngroup=1; % group of electrons jump barrier, initialize to 1 so no divide by zero warning
  groupind=0; % 1 means a group of electrons is waiting to TE, 0 is normal
  k = 1; % index for time, so can of limit no. of time steps which is the Tmeas
  nind=1; % index for checking ngroup
  neTE=0; % total number of electrons TE'd

% % determine if there is bunching
if ( (q/Cdep) < (kB*T/q) ) % q/Cdep is change in jcn voltage from TE,a kT/q is thermal voltage
  bunching = 1;
  nTE=ngroup; % number of electrons last TE'd
else
  bunching = 0;
end

if bunching==1  % bunching occurs, calculate TE the using Poisson & Gaussian
        % this is usually the case, depends mostly on capacitance

nTE=1; % initialize to 1
  while k <  timeSteps

     % Calculate IDS for this time step
     VGS=VG-VS; % gate source voltage
     VDS=VD-VS; % drain source voltage
     VM=VFB+2*Ef+(bodyfactor*sqrt((2*Ef)+VSBprime)); % upper limit of W.I.
     IMprime=nuN*((sqrt(2*q*epsilonSi*NA))/(2*sqrt(2*Ef+VSBprime)))*phiT^2;
     n=1+(bodyfactor/(2*sqrt(2*Ef+VSBprime)));
     % calculate voltage dependent current
```

```
IDS=(W/L)*(IMprime)*(exp((VGS-VM)/(n*phiT)))*(1-exp(-VDS/phiT)); % p. 173
checkIDS(k,:)=IDS; % to debug IDS eqn.

    % Calculate initial TEcondition
    Koft=(Aeff*T^2*Astarrn/e)*(exp((e/(kB*T))*(VS-Vd)));
    TEcondition=Koft*deltaT;
    r1=unifrnd(0,1);  % used to compare to TEcondition to decide if TE occured.
    deltaVS=q/Cdep; % change in voltage from gaining or losing one electron
    r2=unifrnd(0,1); % used to compare to RecombCondition to decide if recombination
occured.

    % decides how many electrons will TE
    nebar=Tmeas*(IDS/q);
    mean=nebar;
    sigma=sqrt(2/r);
    ngroup=randn*sigma+mean;
    ngroup=fix(ngroup); % rounds ngroup to an integer toward zero
    checkngroup(k,:)=ngroup;
    lambda=1; % on average in one time step, one electron will TE

    % Check for TE
    if (TEcondition > r1) % TE will occur
      numTimesTE=numTimesTE+1;
      VS=VS-(n*deltaVS); % group of e-s go so drop jcn voltage
      my_voltage(k,:)=VS; % voltage for this time step

      n=n+ngroup;
      Koft=(Aeff*T^2*Astarrn/e)*(exp((e/(kB*T))*(VS-Vd)));
      TEcondition=Koft*deltaT;
      time(k,:) = t; % array of all time steps (s)
      t=t+deltaT; % go to next time
      k=k+1; % increments the time step
      nTE=ngroup; % for next loop, the number of elec. last TE'd
    else % no TE occurs
      nladd=6.24e18*deltaT*IDS; % number of electrons to add from the current when no
TE occurs
      nladd=round(nladd); % rounds nladd to nearest integer
      deltaVS=nladd*q/Cdep; % change in junction voltage due to the current
      VS=VS+deltaVS; % increase junction voltage since no TE
      my_voltage(k,:)=VS; % voltage for this time step
      % Recalculate TE rate
      Koft=(Aeff*T^2*Astarrn/e)*(exp((e/(kB*T))*(VS-Vd)));
      checkn(k,:)=n; % for debugging
      time(k,:) = t;
```

```
            t = t + deltaT; % go to next time step
            k=k+1;
          end
   % check different variables for debugging.
   checkTEcondition(k,:)=TEcondition; % for debugging TE condition
   checkKoft(k,:)=Koft; % for debugging TE condition
   checkr1(k,:)=r1; % for debugging TE condition
   checkr2(k,:)=r1; % for debugging TE condition
   checkTEif(k,:)=(TEcondition)-r1; % for debugging TE condition
   end % end of while loop for no bunching
end % end of if bunching==0 statement

hivoltage=max(my_voltage);

%%%%%%%%%%%%%%%%%%%%%%%%%%%%%%%%%%%%%%%%%%%%%%%%%%%%%
% plot the data

figure(1);
plot(time,my_voltage);
xlabel('time (sec)');
ylabel('voltage (V)');
title('C=1 fF, R=3k ohm');

figure(2);
hist(checkngroup,20);
xlabel('ngroup value');
ylabel('Number of Occurences')
title('Histogram of ngroup');
```

TEpnkTC.m

```
% Filename: TEpnkTC.m
% Written by: Irene Calizo Feb 2005
% Last Revised: 19-June-2005 morning
% San Jose State University
%
% REQUIREMENTS:
%
% Toolboxes: Statistics
% Other m-files: none
% Other files: none
% Functions:  none
% Subfunctions: None
%
% This script performs a Monte Carlo simulation for reset noise in CMOS
% image sensor pixel
% --------------------------------------------------------------------

clear all;

% **** CONSTANTS *** %
% Planck's Constant (eV*s)
h = 4.14*10^-15;
% Boltzmann's constant
kB=1.38e-23;
% Thermal voltage (at 300K)
kToverq=0.0259; % (V)
phiT=kToverq;
kT = 0.026; % (eV)
% electron charge (C)
q = 1.6*10^(-19);
e = 1.6*10^(-19);
% Free electron mass from cover of Yang (kg)
m=9.1e-31;
% electron effective mass for Si from Yang
me=0.22*m;
% electron mobility in Si (cm^2 / V*s)
%un=1450;
% Effective density of states in the conduction band for Silicon
Nc=2.86*10^19;
% Intrinsic carrier concentration (cm-3)
ni = 9.65*10^9;
% Permittivity in vacuum (F/cm)
```

```
epsilonNot=8.85*10^-14;
% Dielectric constant of Silicon
kSi=11.9;
% dielectric constant of oxide
kox=3.9;
% Silicon permittivity (F/cm)
epsilonSi=kSi*epsilonNot;
% Oxide permittivity
epsilonox=kox*epsilonNot ;
% electron mobility
nuN=1450; % cm^2/V*S

% **** SETTINGS *** %
% Transistor sizing (cm)
W=1e-2 ; % 100 um
L= 5e-4; % 5 um
% Impurity doping concentrations(cm-3)
ND = 10^15;
NA = 10^17;
% Oxide thickness (cm)
tox=1e-6; % 100A=10nm=1e-6cm
% Band digram info
Ec_2_Ef=kT*log(Nc/ND);
Ef_2_Ei=kT*log(ND/ni);
% Ei = 0;
Ef=Ef_2_Ei;
Ec=Ef+Ec_2_Ef;
% Capacitance of diode
Cdep=1e-15; % farads
% Series Resistance
Rs=3e3;
% Built in potential (eV)
Vbi=kT*log( (ND*NA)/ni^2 ) + Ef;  % This is relative to Ei so must add Ef
% Effective built-in potential (eV)
Vd=Vbi+(e^2/(2*Cdep));
% p-region x-sectional area
A=1;
% Number of time steps to take for jcn voltage vs. time plot
timeSteps=200;
% Effective cross-sectional area of n-type layer (um^2)
Aeff=1;
% Temperature (K)
T=300;
% Richardson's constant (A/K^2-cm^2) for n and p-type Silicon
```

```
Astarrn=100;
% Time Step (sec)
deltaT=1e-9;
% parameter for the ratio of single-electron charging energy and the
%   characteristic energy of thermal fluctuation
r = ((q^2)/(Cdep*kB*T));

% **** RESET TRANSISTOR PARAMETERS *** %
% oxide cap. per unit area
Coxprime=epsilonox/tox;
% Effective interface charge per unit area (C/cm2)
Qnotprime=1e-8;
% Contact potential
phiMS=-Ef-0.56;
% Flatband voltage
VFB= phiMS-(Qnotprime/Coxprime);
% Body effect coefficient
bodyfactor=5.8e-16*sqrt(NA)/Coxprime;
% Fixed source body voltage
VSBprime=1;
% Source voltage
VS=0; % Initially zero 0V
% Threshold voltage of reset transistor
VTR=0.7;
% Drain voltage
VD=0.1;
% Gate voltage
VG=0.1;
% Gate Source voltage
VGS=VG-VS;
% Drain Source voltage
VDS=VD-VS ;
% Upper limit of weak inversion
VM=VFB+2*Ef+(bodyfactor*sqrt((2*Ef)+VSBprime)); % upper limit of W.I.
% Current at VM
IMprime=nuN*((sqrt(2*q*epsilonSi*NA))/(2*sqrt(2*Ef+VSBprime)))*phiT^2;
% Inverse slope of surface potential in weak inversion vs. VGB
n=1+(bodyfactor/(2*sqrt(2*Ef+VSBprime)));
% calculate voltage dependent current
%% Source referenced model of MOS transistor in weak inversion
IDS=(W/L)*(IMprime)*(exp((VGS-VM)/(n*phiT)))*(1-exp(-VDS/phiT)); % p. 173 Tsividis
IDSo=IDS; % initial current value with VS=0V

% **** THERMIONIC EMISSION SETTINGS *** %
```

```
% single electron charging time aka tau
tau = q/IDS;
% thermionic emission time aka tauTE
tauTE = tau/r;
% Ktime is t in the K(t) eqn
Ktime=deltaT; % should be equal to deltaT
% Measurement time
Tmeas=1e-6;
% Max number of electrons can get from current per unit time
nmax=Tmeas*(IDS/q);
% average number of electrons that are TEd
nebar=Tmeas*(IDS/q);

% **** INITIALIZATIONS *** %
t=0; % initialize time
jj=1;

%%%%%%%%%%%%%%%%%%%%%%%%%%%%%%%%%%%%%%%%%%%%%%%%%%%
%%%%%%%%%%%%%%%%%%%%%%%%
for jj=1:1:1000 % number of trials too keep track of

   VSo=IDSo*Rs; % initial junction voltage due to external current (V).
   VS=VSo; % setting for first time step
   n=1; % initial number of electrons
   barrier=Vd-VS; % barrier to TE
   ngroup=1; % group of electrons jump barrier, initialize to 1
   k = 1; % index for time, sets # of time steps
%     nTE=0; % total number of electrons TE'd

% % determine if electrons are bunching
if ( (q/Cdep) < (kB*T/q) ) %
   bunching = 1;
   nTE=ngroup; % number of electrons last TE'd
else
   bunching = 0;
end

if bunching==1  % bunching occurs, calculate TE the using Poisson & Gaussian
nTE=1; % initialize to 1
numTimesTE=0; % number of times in one trial that TE occurs
   while k <  timeSteps

      % Calculate IDS for this time step
      VGS=VG-VS; % gate source voltage
```

```
VDS=VD-VS; % drain source voltage
VM=VFB+2*Ef+(bodyfactor*sqrt((2*Ef)+VSBprime)); % upper limit of W.I.
IMprime=nuN*((sqrt(2*q*epsilonSi*NA))/(2*sqrt(2*Ef+VSBprime)))*phiT^2;
n=1+(bodyfactor/(2*sqrt(2*Ef+VSBprime)));
% calculate voltage dependent current
IDS=(W/L)*(IMprime)*(exp((VGS-VM)/(n*phiT)))*(1-exp(-VDS/phiT)); % p. 173
checkIDS(k,:)=IDS; % to debug IDS eqn.

    % Calculate initial TEcondition
    Koft=(Aeff*T^2*Astarrn/e)*(exp((e/(kB*T))*(VS-Vd)));
    TEcondition=Koft*deltaT;
    r1=unifrnd(0,1);  % used to compare to TEcondition to decide if TE occured.
    deltaVS=q/Cdep; % change in voltage from gaining or losing one electron
    r2=unifrnd(0,1); % used to compare to RecombCondition to decide if recombination
occured.

    % decides how many electrons will TE
    nebar=Tmeas*(IDS/q);
    mean=nebar;
    sigma=sqrt(2/r);
    ngroup=randn*sigma+mean;
    ngroup=fix(ngroup); % rounds ngroup to an integer toward zero
    checkngroup(k,:)=ngroup;
    lambda=1; % on average in one time step, one electron will TE

    % Check for TE
    if (TEcondition > r1) % TE will occur
      numTimesTE=numTimesTE+1;
      checknumTimesTE(k,:)=numTimesTE;
      VS=VS-(n*deltaVS); % group of e-s go so drop jcn voltage
      my_voltage(k,:)=VS; % voltage for this time step

      n=n+ngroup;
      Koft=(Aeff*T^2*Astarrn/e)*(exp((e/(kB*T))*(VS-Vd)));
      TEcondition=Koft*deltaT;
      time(k,:) = t; % array of all time steps (s)
      t=t+deltaT; % go to next time
      k=k+1; % increments the time step
      nTE=ngroup; % for next loop, the number of elec. last TE'd
    else % no TE occurs
      nladd=6.24e18*deltaT*IDS; % number of electrons to add from the current when no
TE occurs
      nladd=round(nladd); % rounds nladd to nearest integer
      deltaVS=nladd*q/Cdep; % change in junction voltage due to the current
```

```
            VS=VS+deltaVS; % increase junction voltage since no TE
            my_voltage(k,:)=VS; % voltage for this time step
            % Recalculate TE rate
            Koft=(Aeff*T^2*Astarrn/e)*(exp((e/(kB*T))*(VS-Vd)));
            checkn(k,:)=n; % for debugging
            time(k,:) = t;
            t = t + deltaT; % go to next time step
            k=k+1;
          end
            % check different variables for debugging.
    checkTEcondition(k,:)=TEcondition; % for debugging TE condition
    checkKoft(k,:)=Koft; % for debugging TE condition
    checkr1(k,:)=r1; % for debugging TE condition
    checkr2(k,:)=r1; % for debugging TE condition
    checkTEif(k,:)=(TEcondition)-r1; % for debugging TE condition
      end % end of while loop for bunching
    end % end of if bunching==1 statement

if bunching==0 % bunching doesn't occur
  while k <  timeSteps
          % decides whether TE will occur
          Koft=(Aeff*T^2*Astarrn/e)*(exp((e/(kB*T))*(VS-Vd)));
          TEcondition=Koft*deltaT;
          r1=unifrnd(0,1);  % used to compare to TEcondition to decide if TE occured.
          deltaVS=q/Cdep; % change in voltage from gaining or losing one electron
          TEconditionzero=Koftnzero*deltaT;
          r2=unifrnd(0,1); % used to compare to RecombCondition to decide if recombination
occured.
  if (TEcondition > r1) % TE will occur
          VS=VS-deltaVS; % one electron goes so drop jcn voltage
          my_voltage(k,:)=VS; % voltage for this time step
          % recalculate Koft & TEcondition
          Koft=(Aeff*T^2*Astarrn/e)*(exp((e/(kB*T))*(VS-Vd)));
          TEcondition=Koft*deltaT;
          time(k,:) = t; % array of all time steps (s)
          t=t+deltaT; % go to next time
          k=k+1; % increments the time step
          n=n+1; % add another electron to TE current
          nTE=1; % for next loop, the number of electrons last TE'd
  else % no TE occurs
          nIadd=6.24e18*deltaT*I; % voltage from no. of electrons to add from the current when no
TE occurs
          deltaVS=nIadd*q/Cdep; % change in junction voltage due to the current
          VS=VS+deltaVS; % increase junction voltage since no TE
```

```
            my_voltage(k,:)=VS; % voltage for this time step
            % Recalculate TE rate
            checkn(k,:)=n; % for debugging
            time(k,:) = t;
            t = t + deltaT; % go to next time step
            k=k+1;
    end
    % check different variables for debugging.
    checkTEcondition(k,:)=TEcondition; % for debugging TE condition
    checkKoft(k,:)=Koft; % for debugging TE condition
    checkr1(k,:)=r1; % for debugging TE condition
    checkr2(k,:)=r1; % for debugging TE condition
    checkTEif(k,:)=(TEcondition)-r1; % for debugging TE condition
    end % end of while loop for no bunching
end % end of if bunching==0 statement

    % values for plotting characteristics of each plot from
    hivoltage(jj,:)=max(my_voltage);
    lovoltage(jj,:)=min(my_voltage);
    trialnum(jj,:)=jj;
    hihist=hist(hivoltage,10);
    lohist=hist(lovoltage,10);

end % end of for jj loop for the 100 trials

stdevhivolt=std(hivoltage) % simulated kTC noise
kTCnoise=sqrt(kB*T/Cdep)  % calculated (theoretical value)
percent_diff_kTC=((kTCnoise-stdevhivolt)/kTCnoise)*100

figure(1);
hist(hivoltage,20);
xlabel('Bins');
ylabel('Voltage')
title('Histogram of High Voltages');

figure(3);
plot(trialnum,hivoltage);
xlabel('Trial Number');
ylabel('High voltage (V)');
title('Highest Voltage for each Simulation (C=1 fF, R=3kohm)');
```

References

[1] H.-S. Wong, "Technology and Device Scaling Considerations for CMOS Imagers," *IEEE Trans. Electron Devices*, vol. 43, no. 12, pp. 2131-2142, Dec. 1996.

[2] B. Pain, G. Yang, M. Ortiz, C. Wrigley, B. Hancock, and T. Cunningham, "Analysis and enhancement of low-light level performance of photodiode-type CMOS active pixel imagers operated with sub-threshold reset," in *Proc. IEEE Workshop on Charge Coupled Devices and Advanced Image Sensors* (Nagano, Japan, June10-12, 1999, pp. 140-143).

[3] J. Lai and A. Nathan, "Reset noise in active pixel image sensors," *Journal of Vacuum Science and Technology A: Vacuum, Surfaces and Films*, vol. 22, no. 3, pp. 987-990, May 2004.

[4] A. Leon-Garcia, *Probability and Random Processes for Electrical Engineering*, Reading, MA: Addison-Wesley Publishing Company, 1994, pp. 84-172.

[5] F. Reif, *Fundamentals of Statistical and Thermal Physics*, New York: McGraw Hill, 1965, pp. 4-40.

[6] Y. Yamamoto, "EE/AP 248: Fundamentals of Noise Processes, Class Notes," [Online document], Sept.2004, Available: http://www.stanford.edu/~sanaka/flink/EEAP248/EEAP248.html

[7] H. Tian, B. Fowler, and A. El Gamal, "Analysis of Temporal Noise in CMOS Photodiode Active Pixel Sensor," *IEEE J. of Solid-State Circuits*, vol. 36, no. 1, pp. 92-101, Jan. 2001.

[8] B. Fowler, M. D. Godfrey, J. Balicki, and J. Canfield, "Low Noise Readout using Active Reset for CMOS APS," in *Proc. SPIE*, vol. 3965, San Jose, CA, Jan. 2000, pp. 126-135.

[9] R. Sarpeshkar, T. Delbrück, and C. A. Mead, "White Noise in MOS Transistors and Resistors," *IEEE Circuits Devices Mag.*, vol. 9, issue 6, pp. 23-29, Nov. 1993.

[10] F. Hooge, "1/f Noise Sources," *IEEE Trans. Electron Devices*, vol. 41, no. 11, pp. 1926-1935, Nov. 1994.

[11] A. van der Ziel, *Noise in solid state devices and circuits.* New York: Wiley, 1986.

[12] M.J. Buckingham, *Noise in electronic devices and systems.* New York: Halsted Press, 1983.

[13] J. Janesick and G. Putnam, "Developments and Applications of High-Performance CCD and CMOS Imaging Arrays," in *Annu. Rev. Nucl. Part. Sci.*, Dec. 2003, pp. 263-399.

[14] A. El Gamal and H. Eltoukhy, "CMOS Image Sensors," *IEEE Circuits Devices Mag.*, vol. 21, no. 3, pp. 6-19, May-June 2005.

[15] R. M. Guidash, T.-H. Lee, P. P. K. Lee, D. H. Sackett, C. I. Drowley, M. S. Swenson, L. Arbaugh, R. Hollstein, F. Shapiro, and S. Domer, "A 0.6 um CMOS Pinned Photodiode Color Imager Technology," in *IEEE Int. Electron Device Meeting Tech. Dig.*, Dec. 1997, pp. 927-929.

[16] A. Imamoglu and Y. Yamamoto, "Noise Suppression in Semiconductor *p-i-n* Junctions: Transition from Macroscopic Squeezing to Mesoscopic Coulomb Blockade of Electron Emission Processes," *Physical Review Letters*, vol. 70, no. 21, pp. 3327-3330, May 1993.

[17] A Imamoglu, Y. Yamamoto, and P. Solomon, "Single-electron thermionic-emission oscillations in p-n microjunctions," *Physical Review B*, vol. 46, no. 15, pp. 9555-9563, Oct. 1992.

[18] A. Hull and N. Williams, "Determination of Elementary Charge E from Measurements of Shot-Effect," *Physical Review*, vol. 25, pp.147-173, Feb. 1925.

[19] Y. Tsividis, *Operation and Modeling of The MOS Transistor*. New York, NY: Oxford University Press, 1999, pp. 170-175.